DOE/ER/13865-115

SYNTHESIS AND CHARACTERIZATION OF NOVEL LANTHANIDE- AND ACTINIDE-CONTAINING TITANATES AND ZIRCONO-TITANATES; RELEVANCE TO NUCLEAR WASTE DISPOSAL

A Dissertation

Presented for the

Doctor of Philosophy

Degree

The University of Tennessee, Knoxville

Shara Leeann Stoddard Shoup

August 1995

DISCLAIMER

Portions of this document may be illegible in electronic image products. Images are produced from the best available original document.

DEDICATION

The author dedicates this work to the glory of God. The Heavenly Father has opened many doors so that this accomplishment could be made and provided the author with the strength to walk through them. May His will continue to be followed throughout her life.

IN MEMORIAM

This dissertation is in memory of the author's grandfather, Edward Oakley Barrett, who passed away during her third year of graduate school. In his own way, he was always very interested in her work and was quick to ask about it.

ACKNOWLEDGMENTS

The author would like to express her deep appreciation to Dr. Carlos Bamberger of the Oak Ridge National Laboratory for the research opportunities he has afforded her and for his role as a mentor which has been an invaluable experience. The author would also like to thank her UT advisor, Dr. Joseph Peterson, for financial support, advice, and the opportunity to participate in research at the Oak Ridge National Laboratory.

The staff at both the University of Tennessee at Knoxville and the Oak Ridge National Laboratory, especially the Transuranium Research Laboratory, are thanked for their support and cooperation needed in the completion of this work. Dr. Richard Haire is acknowledged for providing some of the XRD data. Tamara J. Haverlock and C. Leigh Kay are thanked for the leachate data obtained by ICP spectrometry and gross alpha counting, respectively. Jennifer Tyree is acknowledged for her help in preparing some of the zirconotitanate compounds. Others thanked for their contributions to this work through their advice and assistance are Elijah Johnson, Shelby Morton, Bruce Moyer, Charley Ray, Bryan Sales, Eliot Specht, and Jim Treen.

The author also wishes to thank the other members of her committee, Dr. Earl Wehry, Dr. Ben Xue, and Dr. Otto Kopp, for their aid and cooperation.

The author wishes to thank her fellow group members and friends met through the chemistry department for their unending support, encouragement, and patience. These people are C. Leigh Kay, Dr. Jerry Burns, Dr. Nathan Stump, Dr. Lester Pesterfield, Randy Hayes, Norman Bores, Eric Bliss, Dr. Wu Xu, Dr. Gang Chen, Joey Hatcher, Kathy Dowlen, Hong Guan, Kirsten and Ned Wolpert, and Jane Doll.

Gratitude is extended to Mrs. Pat Lancaster, the author's high school chemistry teacher, for the exciting introduction to chemistry that initiated the author's interest in this subject. The Chemistry Department at the University of Tennessee at Chattanooga, especially Dr. Greg Grant, is greatly appreciated for the educational and research experiences received there.

Last, but definitely not least, the author would like to thank her husband, Ryan, parents, Ernest and Sandra, the rest of her family, and her church family for their continuous support, understanding, interest, and encouragement. This work could not have been completed without them.

This research was sponsored in part by the Division of Chemical Sciences, U.S. Department of Energy under grant DE-FG05-88ER13865 to the University of Tennessee at Knoxville and contract DE-AC05-84OR21400 with Lockheed Martin Energy Systems, Inc., the manager of the Oak Ridge National Laboratory for the U.S. Department of Energy.

ABSTRACT

Because working with actinide elements requires special facilities for handling them, many compounds of these elements are less-well studied than those of non-radioactive elements. Thus, augmenting the knowledge about actinide compounds has intrinsic scientific and technological values. For example, investigations of several actinide compounds, which are discussed here, have potential applications such as immobilization matrices for nuclear wastes.

However, before experiments using actinide elements are performed, synthetic routes are tested using lanthanides of comparable ionic radii as surrogates. Compound and solid solution formation in several lanthanide-containing titanate and zircono-titanate systems have been established using X-ray diffraction (XRD) analysis, which helped to define interesting and novel experiments, some of which have been performed and are discussed, for selected actinide elements. The aqueous solubilities of several lanthanide- and actinide-containing compounds, representative of the systems studied, were tested in several leachants, including the WIPP "A" brine, following modified Materials Characterization Center procedures (MCC-3). The WIPP "A" brine is a synthetic substitute for that found in nature at the Waste Isolation Pilot Plant (WIPP) in New Mexico.

The concentrations of cerium, used as a surrogate for

plutonium, leached by the WIPP "A" brine from all the cerium-containing compounds and solid solutions tested were below the Inductively Coupled Plasma (ICP) atomic emission spectrometry limit of detection (10 ppm) established for cerium in this brine. The concentrations of plutonium leached from the two plutonium-containing solid solutions were less than 1 ppm as determined by gross alpha counting and alpha pulse height analysis. Concentrations of strontium leached by the WIPP brine from stable strontium-containing titanate compounds, studied as possible immobilizers of both ^{90}Sr and actinide elements, were also quite low.

These compound and solid solution formation investigations and the aqueous solubility studies suggest that the types of titanate and zircono-titanate compounds and solid solutions studied in this work appear to be useful as host matrices for nuclear waste immobilization.

TABLE OF CONTENTS

LIST OF TABLES

LIST OF FIGURES

CHAPTER I

INTRODUCTION

A. Background on the Lanthanides and Actinides

At the bottom of the periodic table lie the largest naturally-occurring group of elements, the lanthanides, and the largest group of synthetic elements, the actinides. One might be led to believe initially that because of this difference in origin there would be few similarities between these two groups, but often times the lanthanides serve as surrogates for the actinides in the study of properties and compound formation, because both groups fill f electron orbitals.

The term lanthanides refers to the elements with atomic numbers 57 through 71, lanthanum through lutetium. Scandium and yttrium are sometimes included in this group because of their comparable ionic radii. All of the lanthanides are known to occur naturally, found in minerals, including unstable promethium (Pm-147, $t_{½}$=2.62 y) which is found in uranium ores [1]. Promethium will not be considered further here in any of the discussion concerning compound formation of the lanthanides.

The lanthanides are the first group of elements that starts to fill an f electron subshell. Therefore, their electronic configurations are that of xenon plus a filled 6s

subshell and different numbers of 4f and 5d electrons. The most common oxidation state of the lanthanides is III. Cerium is also known to have a IV oxidation state stable in air at high temperature, and there are several examples of compounds with europium in the II oxidation state.

The ionic radii of the lanthanides in the III oxidation state decrease across the periodic table from La(III) to Lu(III). This is known as the "lanthanide contraction" and occurs because the outer electrons are insufficiently shielded from the nuclear charge by the f electrons.

The term actinides is used to refer to the elements with atomic numbers 89 through 103, actinium through lawrencium. All of these elements are radioactive, and only the elements actinium through uranium occur naturally. Neptunium through lawrencium are "man-made," and their availability decreases generally with increasing atomic number.

The actinides fill the 5f electron subshell which gives rise to electronic configurations of radon plus a filled 7s subshell and different numbers of 5f and 6d electrons. Multiple oxidation states are exhibited by the actinides with IV being a stable state for the elements thorium through plutonium and III the most common state for americium and the rest of the actinides (except for the II oxidation state of nobelium). An "actinide contraction" of the ionic radii similar to the "lanthanide contraction" is

also observed.

B. Background on Lanthanide-Containing Titanates and Zirconates

The lanthanides in the III oxidation state form dititanate compounds with the formula $Ln_2Ti_2O_7$. The crystal structure exhibited by the dititanates of the larger lanthanides, lanthanum through neodymium, denoted here as $Ln_2Ti_2O_7$, is monoclinic, and is considered isostructural with the compound $Ca_2Nb_2O_7$ (space group C_2^2, $P2_1$ (4) or $P2_{1m}$ (11), Z=4) [2]. A schematic of this proposed monoclinic structure for $Ln_2Ti_2O_7$ [2] is given in Figure 1. Preliminary structural studies of $La_2Ti_2O_7$ indicated that the Ti(IV) ions are sixfold coordinated with oxygen forming TiO_6 units, while the La(III) ions are expected to be ninefold coordinated with oxygen forming LaO_9 units [3].

The heavier lanthanide dititanates of samarium through lutetium, denoted here as $Ln'_2Ti_2O_7$, have smaller ionic radii and exhibit a pyrochlore-type structure (space group Fd3m-O_h^7, Z=8) based on the mineral pyrochlore with an approximate formula $(Ca,Na,Ce,Th)_2(Nb,Ta,Ti)_2O_6(OH,F)$ [4]. These lanthanide dititanates follow the generalized formula $A_2B_2O_7$ of the pyrochlore (A=Ln; B=Ti) and have radius ratio values comparable to those observed necessary for pyrochlore-type formation [5], i.e., $1.46 \leq r_A/r_B \leq 1.78$, where r_A and r_B are the ionic radii of elements A and B. A

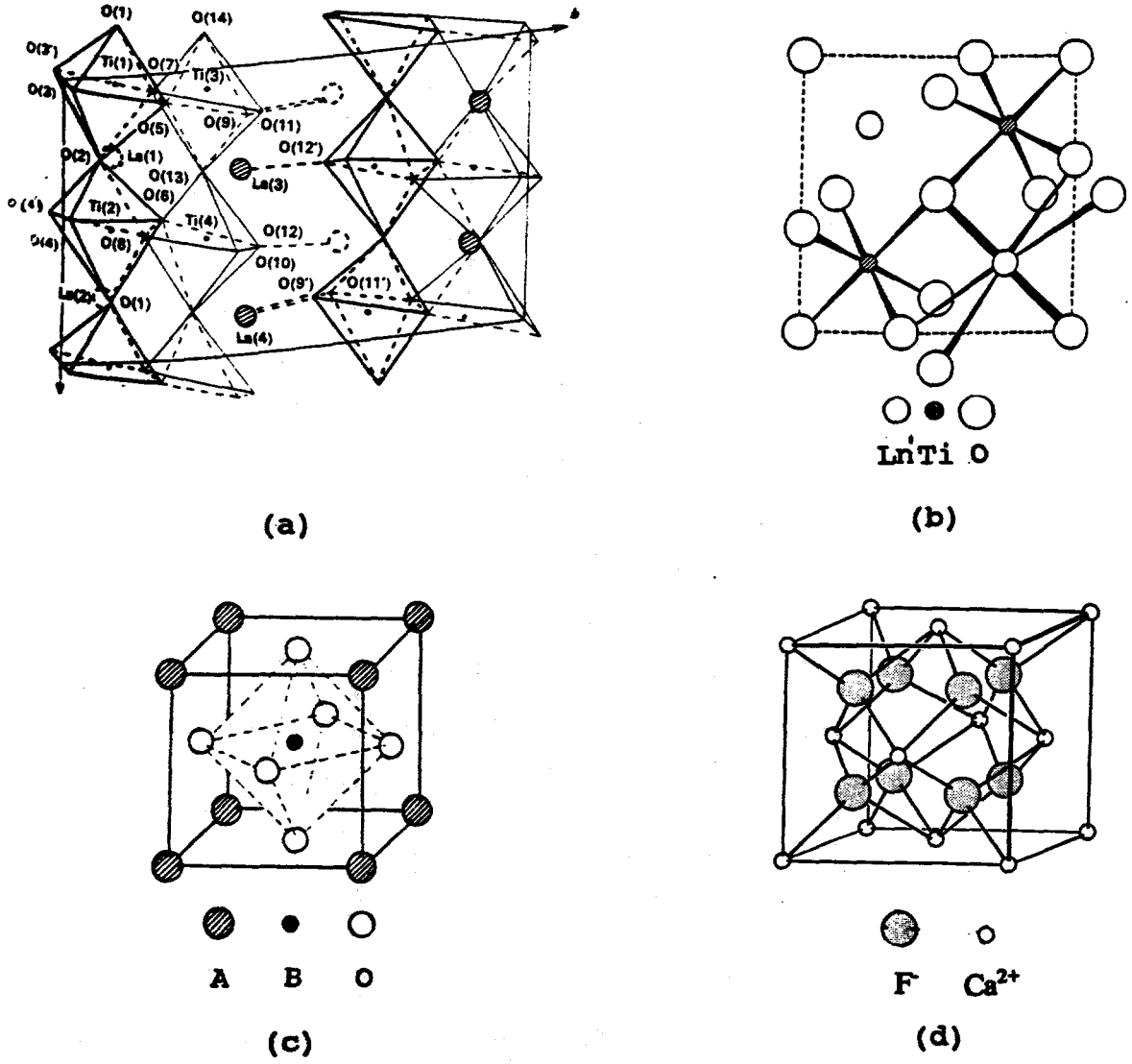

Figure 1. Schematic Structures of (a) Monoclinic $Ln_2Ti_2O_7$, (b) Cubic Pyrochlore-Type $Ln'_2Ti_2O_7$, (c) Ideal Cubic Perovskite ABO_3, and (d) Ideal Fluorite.

schematic of the pyrochlore-type $Ln'_2Ti_2O_7$ structure [5] is given in Figure 1. The Ti(IV) ions form TiO_6 units, while the Ln(III) ions are eightfold coordinated with oxygen (LnO_8 units) [5]. It has been established that there is some solubility between the two types of lanthanide dititanates, $Ln_2Ti_2O_7$ and $Ln'_2Ti_2O_7$ [6,7]. The pyrochlore-type solid solution formation is discussed in more detail in Chapter III, section A.

The titanate systems mentioned above contain Ln(III) and Ti(IV), but there are also other ternary titanate systems known containing some Ti(III) in addition to Ln(III) and Ti(IV) [7-11]. Such compounds have the formula $Ln_2O_3 \cdot (3TiO_{2-m})$ or $Ln_2Ti_3O_{9-3m}$ (Ln=La-Nd, m<0.25) and exhibit a perovskite-type structure. A schematic of an ideal perovskite structure [12] is shown in Figure 1. In an ideal cubic perovskite ABO_3, the A ions are twelve-coordinated, while the B ions form the BO_6 octahedral units [12]. A tolerance factor, $t=(r_A+r_O)/1.414(r_B+r_O)$ where r_A, r_B, and r_O are the ionic radii of elements A, B, and oxygen and with $0.75 < t < 1.00$, has been defined to suggest which compounds will exhibit perovskite-type structures [13].

It has been reported that the structure for $Ln_2Ti_3O_{9-3m}$ has A-site vacancies [11]. These can be better visualized from the formula written as $Ln_{2/3}TiO_{3-m}$ and compared to the formula of the ideal perovskite ABO_3. It has also been reported that the structure is cubic, tetragonal, or

orthorhombic depending on the value of m, which appears to be determined by the reaction temperature and atmosphere [11]. The larger the value of m, the higher the symmetry of the structure [11].

Perovskite-type solid solutions between $Ln_2Ti_3O_{9-3m}$ and the cubic perovskite $SrTiO_3$ ($Sr_{4-x}Ln_{2x/3}Ti_4O_{12}$) are known [14-16]. The structure of the solid solutions is thought to be more complex than that described above with vacancies possibly at both the A- and B-sites [15]; the use of tolerance factors does not accurately determine whether a composition will form the perovskite-type structure in these systems.

Another series of perovskite-type solid solutions known is that of $Sr_{6-12x}Ce_{6x}Ti_5O_{16}$ ($0.08 \leq x \leq 0.43$) [17]. In this system, cerium is in the IV oxidation state in contrast to the above-mentioned systems where the lanthanide is in the III state. The structure of these solid solutions is most likely similar to that of the solid solutions $Sr_{4-x}Ln_{2x/3}Ti_4O_{12}$.

The lanthanides also form dizirconates which have the formula $Ln_2Zr_2O_7$. The lighter lanthanides from lanthanum to gadolinium form cubic pyrochlore-type dizirconates [5], denoted here as $Ln_2Zr_2O_7$, that are of the same space group as the pyrochlore-type dititanates. The remaining, heavier lanthanide dizirconates with radius ratios too small for pyrochlore-type formation exhibit a defect fluorite structure [5]. The ideal fluorite structure, shown in

Figure 1, is that of CaF_2 [18]. The calcium ions are surrounded by four fluoride ions, while the fluoride ions are surrounded by eight calcium ions [18].

Very few cases of mixed titanium-zirconium pyrochlore- or perovskite-type compounds and solid solutions have been reported [19-21]. These systems are discussed in more detail in Chapter V, section A.

The titanates, zirconates, and zircono-titanates discussed above have been previously studied because of their solid solution formation and interesting magnetic, electrical, and optical properties [5-7,15,16,22]. Another, less studied use for these materials is as possible immobilizers of nuclear waste.

C. Background on Nuclear Waste Immobilization Research

The need for immobilizing long-lived radioactive elements in solid matrices was initiated with the uses of these elements as energy sources, medical isotopes, and in military applications [23]. Four major groups of waste forms have been proposed and studied with regard to immobilizing these radioactive elements; these waste form groups are: glasses, ceramics, coated particles, and particles in metal matrices [24]. The most important factor to be considered once a host is found that will immobilize the radioactive elements is the long-term durability of the host with respect to leaching. In early 1978 the United

States Department of Energy (DOE) decided to study the possibility of storing immobilized transuranic nuclear waste in underground salt repositories. Thus was born the Waste Isolation Pilot Plant (WIPP), a mined repository in bedded salt, located in Eddy County, New Mexico (close to Carlsbad). Since that time leaching studies using many leachants have been performed on proposed waste forms, some containing actual radioactive elements and some containing only surrogates, to estimate the solubility and leaching rates of ions in the hosts in the event that a breach by water of such a repository occurred [25-29].

A 1981 report by the Alternative Waste Form Peer Review Panel ranking alternate waste forms listed borosilicate glass as the number one waste form and SYNROC, a titanate-based ceramic, as the number two form but stated that more extensive leaching studies of these materials were needed [30]. Evaluations of these materials are still being carried out today [31].

Borosilicate glasses are the current waste host of choice for most countries including the United States. While glasses can accommodate a wide range of waste stream compositions [24], there is still concern that they will not be as stable as other waste forms during the first several decades of storage should they come in contact with water [32]. Also, there are concerns that not all waste streams could be easily vitrified and that, on a large scale,

chemically and physically homogeneous glasses may be hard to produce [31]. It appears that glasses will serve as a major immobilization matrix for nuclear wastes, but there is still a need for developing other matrices.

Ceramics, such as SYNROC, seek to mimic minerals that have been geologically stable and have retained naturally occurring radioactive elements for millions of years. In SYNROC, the radioactive elements are distributed in three main synthetic minerals: hollandite ($BaAl_2Ti_6O_{16}$), perovskite ($CaTiO_3$), and zirconolite ($CaZrTi_2O_7$) [25,33]. An advantage of such minerals is that they can accommodate many elements in their structures by substitution, covering a range of ionic sizes and valences, which is an important consideration for immobilizing high-level radioactive waste. Leaching studies have indicated that SYNROC and other ceramic materials fare just as well as, if not better than, glasses with respect to leaching rates and long-term durability of the host [25,34].

D. Proposed Course of Research

The aim of this research was to investigate novel compound and solid solution formation in lanthanide- and actinide-containing titanate and zircono-titanate systems using X-ray diffraction. These systems were first studied and defined using the lanthanides as surrogates for the actinides. Finally, the durability, with respect to

leaching, of several representative lanthanide- and actinide-containing compounds was tested in various aqueous leachants to evaluate potential matrices for nuclear waste immobilization.

CHAPTER II

EXPERIMENTAL PROCEDURES

A. Compound Synthesis

1. Reactants Used

The compounds were prepared by dry grinding, using mortar and pestle, the appropriate reactants together in the desired compositions. The lanthanide oxides used were La_2O_3 (ALFA Products), CeO_2 (Fisher Scientific), Pr_6O_{11} (manufacturer unknown), Nd_2O_3 (Michigan Chemical Co.), Gd_2O_3, (REacton), Er_2O_3 (Michigan Chemical Co.), and Lu_2O_3 (GFS Chemicals). All of these were labelled to be at least of 99% purity except for Nd_2O_3, which was labelled 95% pure. The actinide oxides used were NpO_2 (Np-237; $t_{½}=2.14\times10^6$ y), PuO_2 (Pu-242; $t_{½}=3.733\times10^5$ y), and AmO_2 (Am-241; $t_{½}=432.7$ y). These isotopes were synthesized in the High Flux Isotope Reactor (HFIR) at the Oak Ridge National Laboratory as part of the U.S. Department of Energy's program for transuranium element production and research. The transition metal oxides used were TiO_2 (Baker) and ZrO_2 (Matheson) with labelled purities of 99.95% and 99%, respectively. $SrCO_3$ (Johnson-Matthey) was used as the source of SrO and was labelled 99.99% pure. Reducing agents used were TiN (Atlantic Equipment Engineers) and ZrN (Materials Research Corp.). Some mixtures were calcined in Ar (Liquid Air

Corp.) or Ar/4% H_2 (Liquid Air Corp.) to provide, respectively, an inert or reducing atmosphere.

2. Containment

Crucibles and boats made of Al_2O_3 or Pt were used to hold the lanthanide-containing solids for calcinations in air. Only Al_2O_3 containers were used with the lanthanides in inert and reducing atmospheres. For the actinide-containing solids, Pt was preferred for the calcinations in air or Ar, while Al_2O_3, BeO, and ZrO_2 crucibles were used for calcinations in Ar or Ar/4% H_2. Such containment was chosen to avoid the formation of Pt-containing intermetallic compounds in the presence of hydrogen and the diffusion of the actinide reactants into the refractory oxides during calcinations in air.

For radiological safety and health reasons, the actinide-containing mixtures were prepared and calcined in an air-flow glove box which was equipped with a balance, two furnaces, and gas lines that led to cylinders of Ar or Ar/4% H_2 gas located in the laboratory.

3. Calcination Reactions

The calcinations of compounds containing the cations Ce(IV) or Ln(III), excluding Ce(III), Ti(IV) and/or Zr(IV) were performed in air in one of several high temperature furnaces (Rapid Temperature Muffle Furnace, CM Inc., model

1706 FL and programmable Variable Profile Tube Furnaces, Harrop Ind., Inc., models P-16-1-2 and SC-16-3/4-3). Compounds containing Ce(III) and Ti(IV) or Ln(III), Ti(III), and Ti(IV) were calcined in Ar or Ar/4% H_2, respectively, also in high temperature furnaces (High Temperature Tube Furnace, Thermolyne, model F54538CM and programmable Variable Profile Tube Furnaces, Harrop Ind., Inc., model SC-16-3/4-3). The actinide-containing compounds were calcined in air, Ar or Ar/4% H_2 in a vertical, water-cooled, platinum-wound tube furnace (Marshall Furnace Co., model 15329) situated in the glove box. The Ar or Ar/4% H_2 gas used in the calcinations of both the lanthanide- and actinide-containing solids was introduced by gas connections attached to the alumina tubes which held the reactants and were placed in the tube furnaces.

Calcination temperatures ranged from approximately 1200 to 1500°C. To aid the completion of the reactions, each compound was reground, sometimes pressed into pellets (except actinide-containing mixtures) and further calcined several times during its preparation. These treatments were considered completed when the X-ray diffraction patterns of the samples did not change. Total reaction times ranged from several hours to several hundred hours. The lanthanide-containing products calcined in air were cooled rapidly, while all actinide-containing products and the lanthanide-containing products calcined in Ar or Ar/4% H_2

were cooled overnight in the atmosphere in which they had been calcined. The scale of preparations ranged from several milligrams for the actinide-containing products to several grams for some of the lanthanide-containing products.

4. Oxidation Reactions

Oxidation reactions of some lanthanide- or actinide-containing compounds were performed in air between 900 and 1025°C. The uptake of oxygen was measured gravimetrically.

B. X-ray Diffraction Analysis

X-ray diffraction (XRD) analysis was the main characterization technique used in the identification of the compounds studied here.

1. Equipment

XRD data for some of the lanthanide-containing compounds were collected using a diffractometer (PAD V, Scintag) with a solid-state germanium detector using Cu $K_{\alpha 1}$ radiation with a wavelength of 0.154059 nm. The following conditions were used: accelerating potential, 45 kV; filament current, 40 mA; takeoff angle of X-ray tube, 4°; fixed divergence slit, 2 mm; fixed receiving slit, 0.3 mm; scan rate, 1°/min. The samples were mounted on a "zero-background" quartz crystal and were typically approximately

five milligrams in mass.

A second instrument used to collect XRD data from lanthanide-containing compounds was a diffractometer (Bragg-Brentano) equipped with a theta-compensating incident beam divergence slit and a graphite (002) diffracted beam monochromator. Cu $K_{\alpha 1}$ radiation was also utilized, and the scan rate was 1.2°/min. The samples were thinly coated on "zero-background" silicon substrate plates and were typically approximately thirty milligrams in mass. Silicon powder was used as an external standard (a_o=0.53406 nm) to calibrate periodically both diffractometers.

Some XRD data for lanthanide-containing compounds were obtained using an X-ray generator (General Electric, model XRD-6) equipped with a copper target. Nickel foil was used to filter out the Cu K_β radiation. Samples were loaded into 0.3 mm diameter glass or quartz capillaries, which were then placed in Debye-Scherrer-type cameras of 57.3 mm in diameter. Each capillary was covered by a beryllium cup for protection against breakage while the film was being loaded into and removed from the camera. Exposure time was normally two hours at room temperature, and the data were recorded on Kodak film (DEF-392, double emulsion). After developing, the films were read on a film reader (Philips Electronics, Inc.) to determine the positions of the diffraction lines to the nearest 0.05 mm.

All XRD data for the actinide-containing compounds were

obtained using an X-ray generator (Philips Electronics, Inc., XRG 3100), equipped with a molybdenum target (Mo $K_{\bar{a}}$ radiation, $\bar{\lambda}$=0.07107 nm), and Debye-Scherrer-type cameras of 114.6 mm diameter. Zirconium foil was used to filter out the Mo K_{β} radiation. The samples were loaded into thick-walled, hand-drawn silica glass capillaries, and a beryllium cup surrounded each sample when in the camera to protect the capillary. Typical exposure times were approximately one-and-a-half to three hours and were performed at room temperature. The XRD data were recorded on Kodak film (DEF-392, double emulsion). After developing, the films were read in the same manner as described above. Internal calibration standards were not used because many of the preparations made were used to prepare other compounds.

2. Analysis of Powder Diffraction Patterns

Pattern-processing software (Jade, Materials Data Inc., 1994) was used to strip $K_{\alpha 2}$ and locate peaks in the XRD data obtained by the diffractometers for some lanthanide-containing samples.

For the XRD data obtained from lanthanide- and actinide-containing samples using the film technique, a Lotus 2.01 spreadsheet (Lotus Development Corp.) was utilized to calculate two-theta values from the positions of the diffraction lines recorded on the films. These values were then converted into interplanar spacings, d, through

the Bragg equation. No film shrinkage factors were used in the analysis of the data. Intensities of the diffraction lines were estimated visually. For comparable exposure times, the Mo $K_{\bar{\alpha}}$ radiation, used for the actinide-containing samples, gave more intense diffraction lines than did the Cu $K_{\bar{\alpha}}$ radiation, but it had the disadvantage of decreased resolution of the lines. This made the determination of the line positions more difficult, especially in the case of the monoclinic structures. Regardless of the radiation used, there is more limited resolution inherent to the film technique compared to the diffractometers.

Lattice parameters were determined using programs such as a modified version of the LCR-2 least squares program [35]. The errors calculated for each parameter are dependent on a particular data set and are to be used for comparative purposes only. These errors, given at one standard deviation, do not represent the true error associated with each parameter.

C. Solubility Studies

The Materials Characterization Center (MCC) has established a number of procedures specifically designed to determine a compound's solubility or leaching rate under different experimental conditions [36]. Following these procedures makes it possible for direct comparison of results obtained by several research groups. Modified MCC-3

procedures [36] were used in this work to study the solubility of selected compounds and solid solutions. The compounds and solid solutions were in contact with the leachants for eight weeks, a reasonable contact time, based on several other studies [25,34,37].

1. Compound Preparation

Approximately 20 grams of each of the five cerium-containing compounds and solid solutions and 250 milligrams of the two plutonium-containing solid solutions chosen for this study were prepared. Each solid was analyzed by XRD to verify that the desired product had been prepared. Then each cerium-containing product was ground in an agate ball grinder (Spex Industries, Inc., cat. no. 8000) fine enough to be sieved through a 325 mesh nylon screen (44 μm pore size) (Spex Industries, Inc.). The plutonium-containing products were ground with porcelain mortar and pestle and sieved through 325 mesh screens. The cerium-containing products were analyzed again via XRD to insure that grinding had not caused changes such as phase changes or separation of phases. The plutonium-containing solid solutions were not analyzed again after grinding.

2. Leachant Preparation

Four solutions were chosen as leachants: WIPP "A" brine [38], 0.1 M NaCl, 0.1 M HCl, and 6.0 M HCl. The composition

of WIPP "A" brine is given in Table I. The NaCl and HCl solutions were prepared from NaCl (Allied Chemical), labelled 99.5% pure, and concentrated HCl (Baker Analyzed), respectively. The pH of each leachant was measured using a pH meter (Beckman Zeromatic).

The solubility of the cerium-containing compounds and solid solutions was studied in all four of the leachants, while only WIPP "A" brine and 6.0 M HCl solutions were used with the plutonium-containing solid solutions. The ratio 1 g solid/10 mL leachant, as stated in the MCC-3 procedure [36], was used in determining the mass of sample per volume of leachant to be used.

3. Container Preparation

To hold the cerium-containing samples, previously used 90 mL Teflon containers (Savillex Corp.) were thoroughly cleaned following the directions given in the MCC-1 procedures [36] for cleaning used containers. Small Teflon containers (manufacturer unknown) of 5 mL capacity were used to hold the plutonium-containing samples. These containers were new and were cleaned according to the specifications listed in the MCC-3 procedures [36] for cleaning new containers.

4. Temperature Control and Agitation Methods

The solubility of the cerium-containing compounds and

Table I

Approximate Composition of WIPP "A" Brine [38]

Ion	Concentration (mg/L solution)
Li^+	20
Na^+	42000
K^+	30000
Rb^+	20
Cs^+	1
Mg^{2+}	35000
Ca^{2+}	600
Sr^{2+}	5
Fe^{3+}	3
Cl^-	190000
Br^-	400
I^-	10
SO_4^{2-}	3500
HCO_3^-	700
BO_3^{3-}	1200

solid solutions were studied at two temperatures, room temperature and 50°C, while the plutonium-containing solid solutions were studied only at room temperature. The MCC-3 procedures [36] call for constant agitation of the samples at the test temperature. Constant agitation at room temperature was achieved by using magnetic stirring bars and plates. The samples held at 50°C were kept in a water bath equipped with a shaker (Magni Whirl Constant Temperature Bath, Blue M Electric Co., model MSB-1122A-1). Constant temperature and agitation were maintained throughout the test period except for approximately three hours during a general power outage.

5. Leachate Filtering

At the end of the eight-week test period, an approximately 5 mL or 1 mL aliquot of the leachate solution from the cerium- or plutonium-containing solids, respectively, was filtered from each container using a 0.45 μm pore size syringe filter connected to a disposable syringe and needle. This aliquot was transferred to a small polyethylene bottle and analyzed, in the case of the cerium-containing samples, via Inductively Coupled Plasma (ICP) atomic emission spectrometry for the concentration of each element of interest. Plutonium-containing samples were analyzed only for the amount of plutonium present by gross alpha counting and alpha pulse height analysis. Filters and

syringes were warmed to 50°C before the aliquots of leachate held at 50°C were taken. The pH of the cerium-containing leachate from every container was measured at the time of sampling.

6. Analysis by ICP Atomic Emission Spectrometry

The filtered leachates from the cerium-containing solids were analyzed using an ICP atomic emission spectrometer (Thermo Jarrell Ash PolyScan Iris) with an argon plasma excitation source. The following plasma conditions were used: auxiliary gas, 3 psig; RF power, 1150 W; nebulizer pressure, 32.0 psi, nebulizer flush pump rate, 100 rpm; nebulizer analysis pump rate, 100 rpm; relaxation time, 0.0 s. The following wavelengths were used to identify the indicated element: Ce, 413.765 nm; Er, 323.058 nm; Sr, 338.071 nm; Ti, 336.121 nm; and Zr, 343.823 or 349.621 nm. Each sample was analyzed three times to obtain average concentrations of the elements of interest. The sample flush time was between 20.0 and 40.0 s. A 1 ppm yttrium internal standard, detected at 360.073 nm, was used in all analyses. Blanks of every leachant solution prepared were analyzed as well.

7. Gross Alpha Counting and Alpha Pulse Height Analysis

The leachates from the plutonium-containing solids were analyzed by performing a gross alpha count using a gas-flow

proportional counter (Tennelec LB 4000, Oxford Instrument Co.). The instrument, which had a low alpha background (0.2 cpm), was calibrated for gross alpha counting using an Am-241 NIST traceable standard. Each sample was plated onto a stainless steel planchet and counted following the EPA-600/900.0 procedure [39]. The counting time for each sample was twenty minutes. Alpha pulse height analyses were performed on 6.0 M HCl leachates using an alpha spectrometer (Tennelec TC 257, Oxford Instrument Co.) and the Genie-ESP Data Acquisition and Processing System (Canberra, Nuclear Data). The same samples used to obtain the gross alpha counts were used, and the acquisition time for each sample was one hour.

8. Analysis of Remaining Solids by XRD

Solids remaining in the original test containers held at 50°C were analyzed via XRD. The solid remnants were washed with distilled water and isopropyl or methyl alcohol, dried, and examined by XRD to determine if there had been any change in the composition of the solid phase during the course of leaching.

CHAPTER III

TITANATE COMPOUNDS AND SOLID SOLUTIONS

A. Background

The lanthanide dititanate compounds, with the exception of $Ce_2Ti_2O_7$, have been previously, for the most part, well studied [40-44]. The light lanthanide dititanates, $Ln_2Ti_2O_7$ (Ln=La-Nd) exhibit a monoclinic structure, space group $P2_1$ (4) or $P2_{1m}$ (11) [2], while the heavy lanthanide dititanates, $Ln'_2Ti_2O_7$ (Ln'=Sm-Lu) exhibit cubic pyrochlore-type symmetry, space group $Fd3m\text{-}O_h^7$ [4]. It is possible to dissolve certain amounts of the light lanthanide dititanates into the heavy lanthanide dititanates forming substitutional solid solutions, $Ln'_{2-x}Ln_xTi_2O_7$ [6,7]. As shown in Figure 2, for a given $Ln_2Ti_2O_7$ and $Ln'_2Ti_2O_7$, ideally the volume of the cubic pyrochlore-type host increases, following Vegard's Law, from that of the volume of pure $Ln'_2Ti_2O_7$ as $Ln_2Ti_2O_7$ is added. Once the solid solution becomes saturated with $Ln_2Ti_2O_7$, the volume of the solid solution remains essentially constant and the presence of a monoclinic phase (assumed to be $Ln_2Ti_2O_7$), in addition to that of the cubic $Ln'_{2-x}Ln_xTi_2O_7$, is detected in the XRD data. The intersection of the sloped and horizontal lines indicates the point of saturation. It is also very likely that some of the heavy $Ln'_2Ti_2O_7$ dissolves into the light $Ln_2Ti_2O_7$, but determining

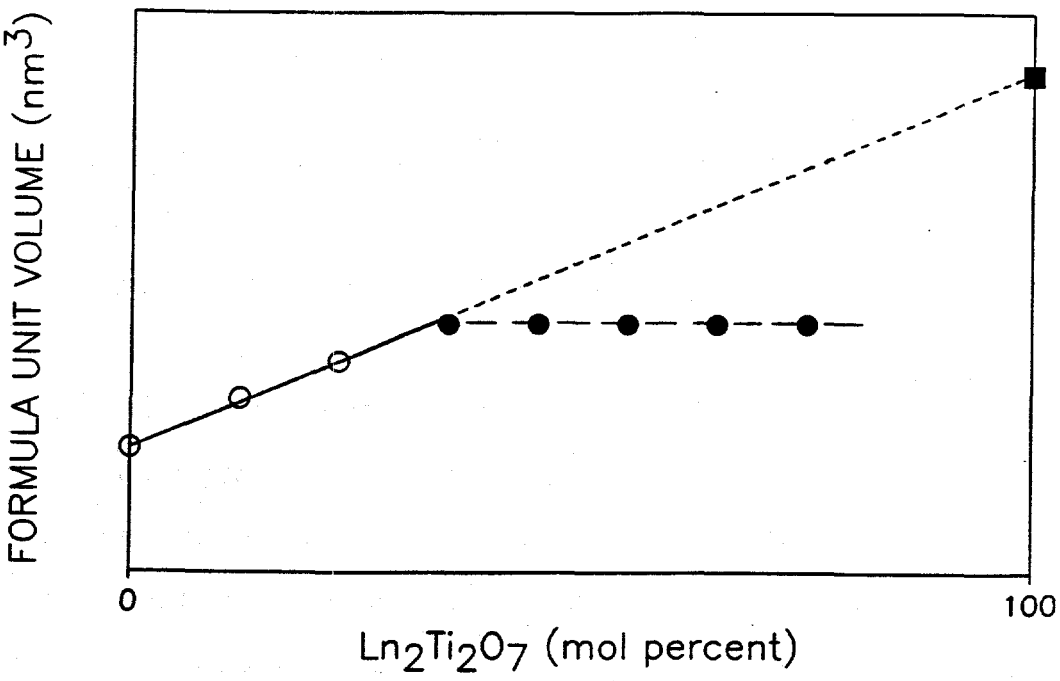

Figure 2. An Ideal Plot of the Solid Solubility of $Ln_2Ti_2O_7$ in Cubic $Ln'_2Ti_2O_7$. Formula Unit Volume of the Cubic $Ln'_{2-x}Ln_xTi_2O_7$ Solid Solution *versus* Mole Percent of $Ln_2Ti_2O_7$ in the Initial Mixture. The Sloped Line Connects the Volume of $Ln'_2Ti_2O_7$ with That of $Ln_2Ti_2O_7$. The Horizontal Line (Filled Circles) Indicates Saturation of the Host Matrix with $Ln_2Ti_2O_7$. The Point of Saturation Is Defined by the Intersection of the Sloped and Horizontal Lines.
O Volume of Unsaturated Cubic Pyrochlore-Type;
● Volume of Saturated Cubic Pyrochlore-Type;
■ Volume of Monoclinic $Ln_2Ti_2O_7$

these solubility limits would be more difficult. It would be hard to detect the presence of excess $Ln'_2Ti_2O_7$, indicating the solid solution was saturated, because there are fewer pyrochlore-type diffraction lines compared to the number from monoclinic $Ln_2Ti_2O_7$, and many of them coincide with those from the $Ln_2Ti_2O_7$ phase.

It was found that as the ionic radius of the heavy, lanthanide ion in the host compound decreased, the solubility of the $Ln_2Ti_2O_7$ increased [6,7]. This can be rationalized using $Sm_2Ti_2O_7$ as the model lanthanide pyrochlore. $Sm_2Ti_2O_7$ has the largest volume of these dititanates; as the radii of the lanthanides beyond samarium decrease, the volume of each pyrochlore-type compound decreases, but the theoretical maximum volume available for a pyrochlore-type lanthanide dititanate remains the same as the volume of $Sm_2Ti_2O_7$. Therefore, when the lanthanide ion Ln' in the host $Ln'_2Ti_2O_7$ is small, the host can dissolve more of a light lanthanide $Ln_2Ti_2O_7$. Of course, there is a maximum volume observed for each saturated $Ln'_{2-x}Ln_xTi_2O_7$ solid solution that is smaller than the volume of $Sm_2Ti_2O_7$ because of factors such as the maximum distance allowable between ions for attraction and bonding to occur. The solid solubility limits of several light lanthanide dititanates, $Ln_2Ti_2O_7$, in several heavy lanthanide dititanates, $Ln'_2Ti_2O_7$, have been experimentally determined and reported [6,7].

Until recently there was a paucity of information about

$Ce_2Ti_2O_7$ and its solid solution formation because of the inert conditions required for working with Ce(III). Cerium is the only lanthanide which exhibits a IV oxidation state stable at high temperature in air. For ease of preparation, researchers had chosen to concentrate on the dititanate compounds of the other lanthanide elements and left the chemistry of Ce(III) dititanate mostly unexplored.

The compound $Ce_2Ti_2O_7$, having monoclinic symmetry, has now been reported [7] by a group in which this author was a member. This Ce(III)-containing compound was easily obtainable following the reaction described in Equation (1).

$$2CeO_2 + 0.5TiN + 1.5TiO_2 \text{ ---> } Ce_2Ti_2O_7 + 0.25N_2 \qquad (1)$$

In this interesting synthesis, TiN was used successfully to reduce Ce(IV) to Ce(III). Calcining in Ar or Ar/4% H_2 resulted in the same brick red compound having no effect on the color or structure of the product. This, therefore, indicated the absence of Ce(IV) or Ti(III).

The solubilities of $Ce_2Ti_2O_7$ in several $Ln'_2Ti_2O_7$ compounds were also determined [7]. The solid solubility limits of $Ce_2Ti_2O_7$ in the cubic pyrochlore-type $Ln'_2Ti_2O_7$ (Ln'=Gd, Er, or Lu) hosts were determined to be 19, 22, and 27 mol percent, respectively [7]. These limits were determined from plots similar to the one shown in Figure 2.

B. Preparation of $An_2Ti_2O_7$ (An=Pu or Am)

The successful synthesis of $Ce_2Ti_2O_7$ led to attempts to prepare $An_2Ti_2O_7$ (An=Np-Am). The compound $Pu_2Ti_2O_7$, blue-black in color, was prepared following the same reaction as described by Equation (1) with plutonium instead of cerium. As for $Ce_2Ti_2O_7$, calcining in Ar or Ar/4% H_2 resulted in the same $Pu_2Ti_2O_7$ product with respect to color and structure. This, therefore, indicated the absence of Pu(IV) or Ti(III). The XRD data from $Pu_2Ti_2O_7$ (Table II) are very similar, as expected, to that from monoclinic $Ce_2Ti_2O_7$ and the other light lanthanide dititanates (Ln=La, Pr, or Nd) acquired using a diffractometer [7,41]. As can be seen in Table II, the number of observed diffraction lines is fewer, and the intensities are higher for some comparable lines of $Pu_2Ti_2O_7$ relative to $Ce_2Ti_2O_7$ [7]. These results reflect the lower resolution of the Mo K_α radiation which results in the close juxtaposition of several lines (e.g., see brackets in Table II) which appear as a single line of higher intensity. For example, the 0.274 nm line in $Pu_2Ti_2O_7$, which exhibited the strongest intensity, is very likely composed (based on the data for $Ce_2Ti_2O_7$ [7]) of the four diffraction lines 410, 020, 212, and -312. The inability to resolve these lines in the XRD pattern from the plutonium compound required the assignment of all four hkl indices to this observed diffraction line when calculating the lattice parameters. The lattice parameters calculated for the monoclinic

Table II

XRD Data Obtained for

Monoclinic $Pu_2Ti_2O_7$ Compared to That for $Ce_2Ti_2O_7$ [7]

$Pu_2Ti_2O_7$			$Ce_2Ti_2O_7$	
Int.	d(nm)	hkl	d(nm)	Int.
m	0.412	210	0.4176	43
m	0.386	002,-102	0.3826	13
		310	0.3378	12
m+	0.312	400	0.3207	61
	0.312	012,-112	0.3150	30
	0.312	202,-302	0.3086	15
m	0.293	112,-212	0.2967	100
s	0.274	410	0.2773	42
	0.274	020	0.2751	37
	0.274	212,-312	0.2692	72
m	0.224	-113	0.2330	6
	0.224	022,-122	0.2235	21
		600	0.2140	12
		412,-512	0.2120	15
w	0.206	420	0.2089	40
	0.206	222,-322	0.2056	16
vw	0.200	610	0.1998	9
m+	0.194	-104	0.1935	44
	0.194	322,-422	0.1915	23
w-	0.189	520,023	0.1878	33
w+	0.175	114,-314	0.1758	15
w+	0.164	330,620	0.1684	10
	0.164	304,-504	0.1662	27
	0.164	132,-232	0.1628	13
m+	0.158	-124	0.1587	17
	0.158	232,-332	0.1579	17
vw	0.153	810	0.1541	12
	0.153	712,-812	0.1506	10
		622,722	0.1484	7

Measured lattice parameters for monoclinic $Pu_2Ti_2O_7$: a_o=1.295±0.008, b_o=0.550±0.003, c_o=0.772±0.004 nm, β=98.5±0.6°; (film, 114.6 mm Ø, Mo $K_{\bar{\alpha}}$ radiation)
Measured lattice parameters for monoclinic $Ce_2Ti_2O_7$ [7]: a_o=1.2985±0.0006, b_o=0.5504±0.0003, c_o=0.7754±0.0004 nm, β=98.58±0.05°; (diffractometer, Cu $K_{\alpha 1}$ radiation)

$Pu_2Ti_2O_7$ using this approach are a_o=1.295±0.008, b_o=0.550±0.003, c_o=0.772±0.004 nm, and β=98.5±0.6°. The volume of the formula unit (four per unit cell) calculated from these parameters is 0.136±0.002 nm^3; it agrees well with the 0.1366 nm^3 determined from the correlation of formula unit volumes [7,41] of $Ln_2Ti_2O_7$ and $Ln'_2Ti_2O_7$ to ion volumes of Ln(III) and Ln'(III) (Figure 3). The ion volumes were calculated using ionic radii for coordination number (CN) = 6. Although the coordination number has been established as 8 for the lanthanide in cubic pyrochlore-type compounds [44], the number is not well established for the monoclinic lanthanide and plutonium compounds. Thus it was elected for consistency in this work to use only the CN=6 values from a single reference [45]. Comparative plots using other CN values did not alter significantly the formula unit volume/ion volume relationship.

Brick-red $Am_2Ti_2O_7$ was prepared directly from AmO_2 and TiO_2. It was not necessary to use TiN to assure reduction. Calcination in Ar between 1200 and 1300°C was sufficient for reducing Am(IV) to Am(III). The compound exhibited monoclinic symmetry which was expected, because the ionic radius of Am(III) is closer to that of Nd(III) than it is to that of Sm(III) [45], the latter being the first lanthanide to exhibit the cubic pyrochlore structure for the dititanate compound. The XRD data for $Am_2Ti_2O_7$ are compared to that for $Nd_2Ti_2O_7$ in Table III. The same procedure used for

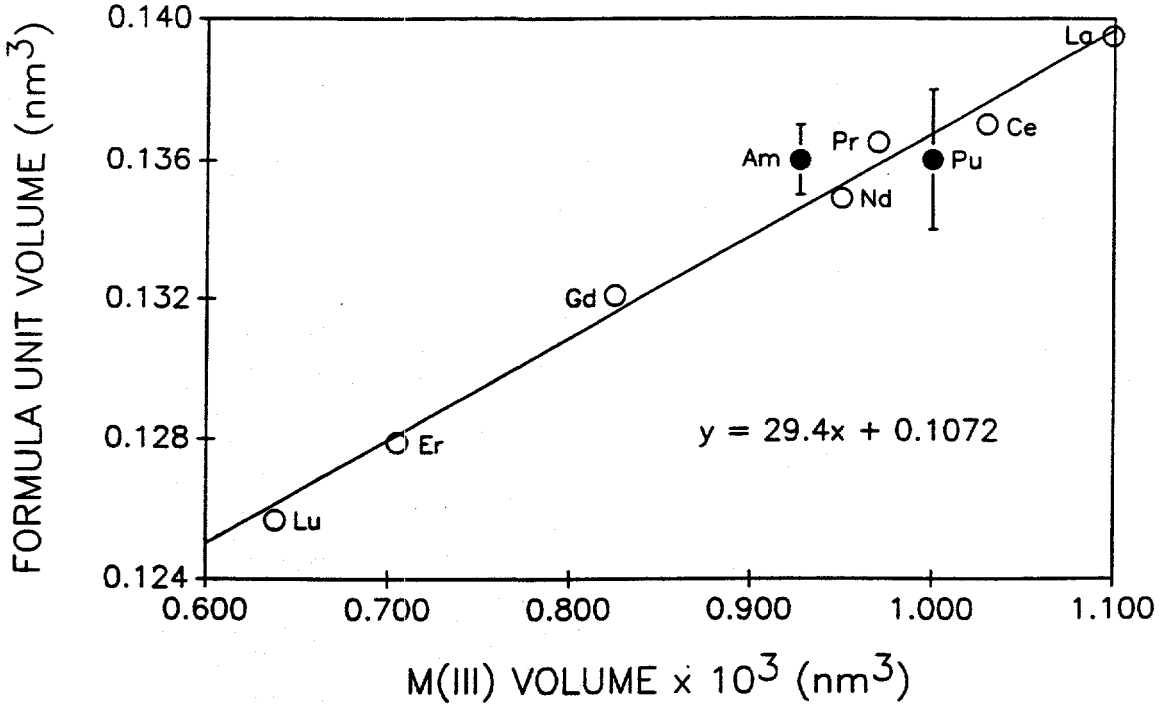

Figure 3. Correlation of Formula Unit Volumes of $Ln_2Ti_2O_7$ and $Ln'_2Ti_2O_7$ to Ion Volumes of Ln(III) and Ln'(III), CN=6 [7,41,45]. The Corresponding Plutonium and Americium Formula Unit Volumes (●) Obtained in This Work Are Included and Are Consistent with This Correlation.

Table III

XRD Data Obtained for

Monoclinic $Am_2Ti_2O_7$ Compared to That for $Nd_2Ti_2O_7$ [41]

$Am_2Ti_2O_7$			$Nd_2Ti_2O_7$	
Int.	d(nm)	hkl	d(nm)	Int.
w+	0.647	200	0.643	9
w	0.505	110	0.5029	5
m+	0.416	210	0.4162	46
m	0.381	002,-102	0.3797	12
		310	0.3372	9
m	0.322	400	0.3216	50
m	0.311	012,-112	0.3119	26
		202,-302	0.3077	13
s	0.295	112,-212	0.2950	100
		410	0.2770	29
		020	0.2732	35
m+	0.267	212,-312	0.2681	50
		302,-402	0.2654	24
vw	0.232	-113	0.2328	6
w+	0.222	022,-122	0.2218	18
vw	0.216	600	0.2154	4
	0.216	412,-512	0.2144	6
w+	0.209	420	0.2082	26
w	0.204	222,-322	0.2043	14
w	0.200	610	0.1996	10
m	0.192	-104	0.1935	44
	0.192	322,-422	0.1915	23
m-	0.188	520,023	0.1878	33
m-	0.175	114,-314	0.1758	15
w	0.168	330,620	0.1684	10
w+	0.165	304,-504	0.1662	27
w+	0.162	132,-232	0.1628	13
m	0.157	-124	0.1587	17
	0.157	232,-332	0.1579	17
		810	0.1541	12
w-	0.151	712,-812	0.1506	10
w	0.148	622,722	0.1484	7

Measured lattice parameters for monoclinic $Am_2Ti_2O_7$:
a_o=1.307±0.003, b_o=0.547±0.001, c_o=0.769±0.001 nm,
β=98.4±0.2°; (film, 114.6 mm Ø, Mo $K_{\bar{\alpha}}$ radiation)
Measured lattice parameters for monoclinic $Nd_2Ti_2O_7$ [41]:
a_o=1.3008±0.0002, b_o=0.54648±0.00007, c_o=0.7679±0.0002 nm,
β=98.56±0.02°; (diffractometer, Cu $K_{\alpha 1}$ radiation)

$Pu_2Ti_2O_7$ was followed in assigning the hkl indices of several unresolved lines to the observed diffraction lines. The lattice parameters of monoclinic $Am_2Ti_2O_7$ using this approach are a_o=1.307±0.003, b_o=0.547±0.001, c_o=0.769±0.001 nm and β=98.4±0.2°. The volume of the formula unit (four per unit cell) calculated from these parameters is 0.136±0.001 nm^3 which agrees well with the value of 0.1345 nm^3 obtained from Figure 3.

The preparative method represented by Equation (1), with neptunium in place of cerium and calcination in Ar/4% H_2, was not conducive to the synthesis of $Np_2Ti_2O_7$. Instead NpO_2 was always detected in the reaction product by XRD. A titanium suboxide should have also been present, to balance the elements in the initial mixture composition, but was not detected in the XRD data, probably because its crystallite size was not sufficiently large and thus did not diffract strongly enough to be seen in the presence of the NpO_2. These results suggest that Np(III) is not stable in this titanate matrix. It was thought that the temperature at which the NpO_2 had been prepared was perhaps too high, rendering the NpO_2 less chemically reactive under the experimental conditions used here, but a "low-fired" source of NpO_2 yielded the same results.

C. $Ln'_{2-x}An_xTi_2O_7$ Solid Solutions (An=Pu or Am)

Dark-colored solid solutions between $Pu_2Ti_2O_7$ and cubic

$Ln'_2Ti_2O_7$ (Ln'=Gd, Er, or Lu) were synthesized by the reaction described by Equation (2).

$$(1-0.5x)Ln'_2Ti_2O_7 + (0.5x)Pu_2Ti_2O_7 \longrightarrow Ln'_{2-x}Pu_xTi_2O_7 \qquad (2)$$

Similarly to previous work with solid solutions of heavy lanthanide dititanates [6,7], the solubility limits of $Pu_2Ti_2O_7$ in $Ln'_2Ti_2O_7$ were determined by analyzing the XRD data from the products for identification of the phases present. The appearance of the monoclinic phase (assumed to be $Pu_2Ti_2O_7$), in addition to the cubic pyrochlore-type phase ($Ln'_{2-x}Pu_xTi_2O_7$), indicated that the cubic host had become saturated with $Pu_2Ti_2O_7$. Lattice parameters and formula unit volumes for the cubic phases present for each composition, including those where excess $Pu_2Ti_2O_7$ was detected, were calculated from the XRD data. These volumes are plotted as a function of the original mole percent of $Pu_2Ti_2O_7$ present in the unfired mixture (Figure 4). Although the plotted data do not yield an ideal plot like that in Figure 2, it can be seen from Figure 4 that, as the $Pu_2Ti_2O_7$ content increases to the point of saturation, the volume of the host cubic $Ln'_2Ti_2O_7$ also increases and should remain constant after saturation. It is interesting to note that the volumes of the plutonium-containing saturated solid solutions appear to be increasing with increasing mole percent $Pu_2Ti_2O_7$ and thus do not exhibit the same ideal plots

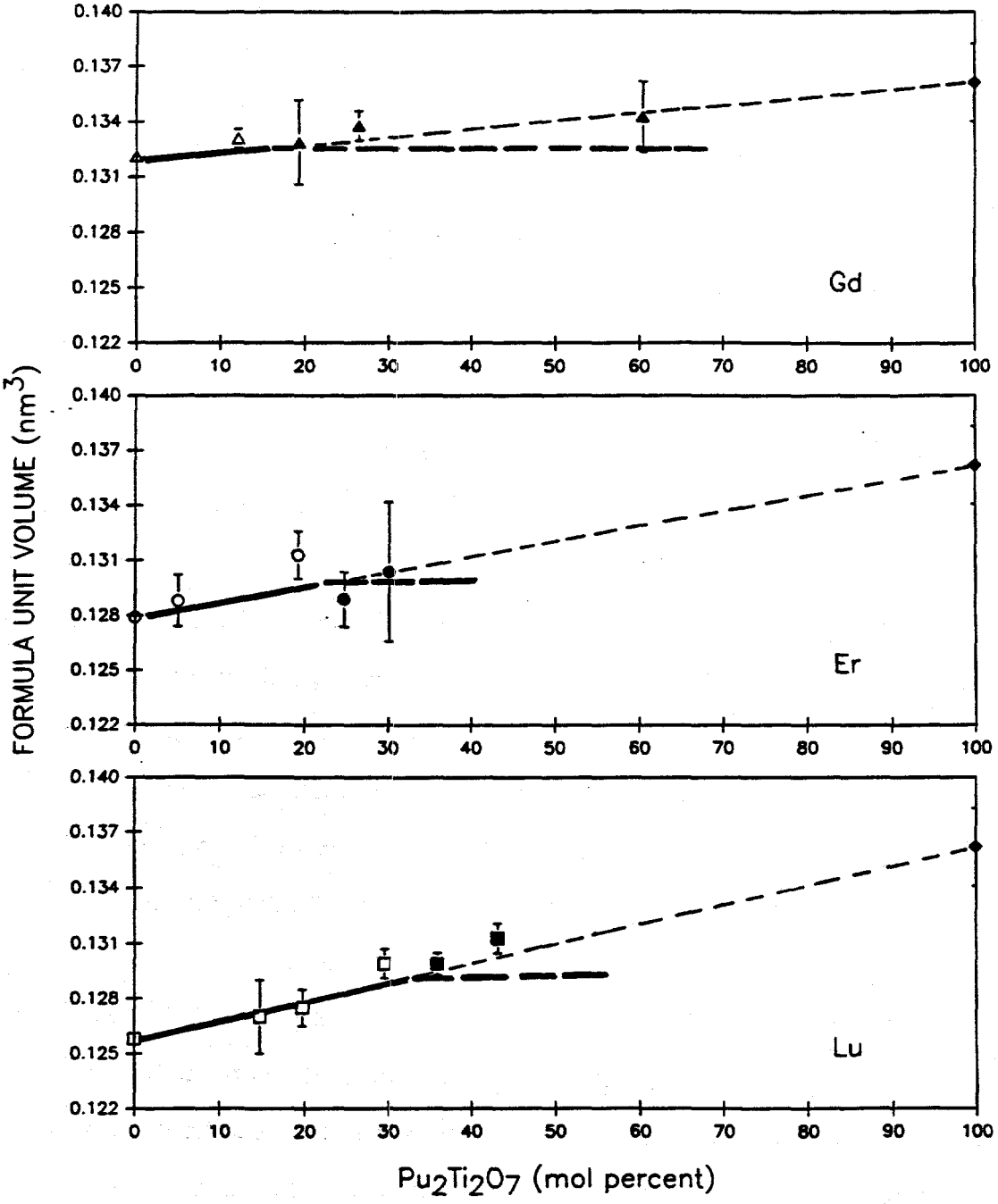

Figure 4. Measured Formula Unit Volume of $Ln'_{2-x}Pu_xTi_2O_7$ versus Mole Percent of $Pu_2Ti_2O_7$ in the Initial Mixture. The Sloped Lines Connect the Volumes of $Ln'_2Ti_2O_7$ with That of $Pu_2Ti_2O_7$. The Horizontal Lines (Filled Symbols) Indicate Saturation of the Host Matrix with $Pu_2Ti_2O_7$. (▲ Gd; ○ Er; □ Lu; ♦ Pu)

expected and seen for the analog cerium-containing solid solutions [7]. This difference may be caused by the fewer data points available for the plutonium-containing systems, larger errors in the calculated formula unit volumes due to the poorer resolution of the diffraction patterns and the use of Mo $K_{\bar{a}}$ radiation, and the possibility that a solid solution rich in $Pu_2Ti_2O_7$, instead of just $Pu_2Ti_2O_7$, is being formed after saturation. This last factor would only decrease the amount of the cubic phase, not change its composition. Future work will be necessary to explain this apparent departure from ideality.

The saturation point is defined for these systems as the composition midway between the last preparation with only a cubic pyrochlore-type solid solution detected in the XRD data and the first preparation showing the presence of a cubic pyrochlore-type solid solution and excess monoclinic $Pu_2Ti_2O_7$ in the XRD data. The horizontal line drawn through the saturated points is not a least squares line and illustrates the solid solution volumes expected based on the saturation point as just defined. As the amount of the monoclinic $Pu_2Ti_2O_7$ increased, the more difficult it became to identify and assign the cubic solid solution lines due to their overlap with the more numerous monoclinic $Pu_2Ti_2O_7$ lines. This limited the number of preparations that could be analyzed unambiguously once saturation with $Pu_2Ti_2O_7$ was exceeded. The solubility limits for $Pu_2Ti_2O_7$ in $Gd_2Ti_2O_7$,

$Er_2Ti_2O_7$, and $Lu_2Ti_2O_7$ (Figure 4) were estimated as 16±4, 22±3, and 33±3 mol percent, respectively. These values agree well with those found for the solubility of $Ce_2Ti_2O_7$ in these same cubic $Ln'_2Ti_2O_7$ hosts (19, 22, and 27 mol percent, respectively) [7].

Brick-red solid solutions between $Am_2Ti_2O_7$ and $Er_2Ti_2O_7$ were prepared using the same type of reaction described in Equation (2). Because of the high specific activity of the americium, and therefore the need to limit the time of exposure to its radiation, especially to the hands, the number of preparations was curtailed to only solid solutions with $Er_2Ti_2O_7$. $Er_2Ti_2O_7$ was selected over $Gd_2Ti_2O_7$ and $Lu_2Ti_2O_7$ because erbium is located between gadolinium and lutetium in the periodic table and would, therefore, represent an "average" solubility of $Am_2Ti_2O_7$ in the three dititanates studied in this work.

The solubility data obtained for the system $Am_2Ti_2O_7$-$Er_2Ti_2O_7$ (see Figure 5) do not make an ideal plot like that depicted in Figure 2. This non-ideal behavior can be addressed in a way similar to that described above for the case of the $Pu_2Ti_2O_7$ solid solutions. The appearance of the monoclinic phase (assumed to be $Am_2Ti_2O_7$), in addition to the cubic pyrochlore-type phase ($Er_{2-x}Am_xTi_2O_7$), indicated that the cubic host had become saturated with $Am_2Ti_2O_7$. Lattice parameters and formula unit volumes for the cubic phases present for each composition, including those where excess

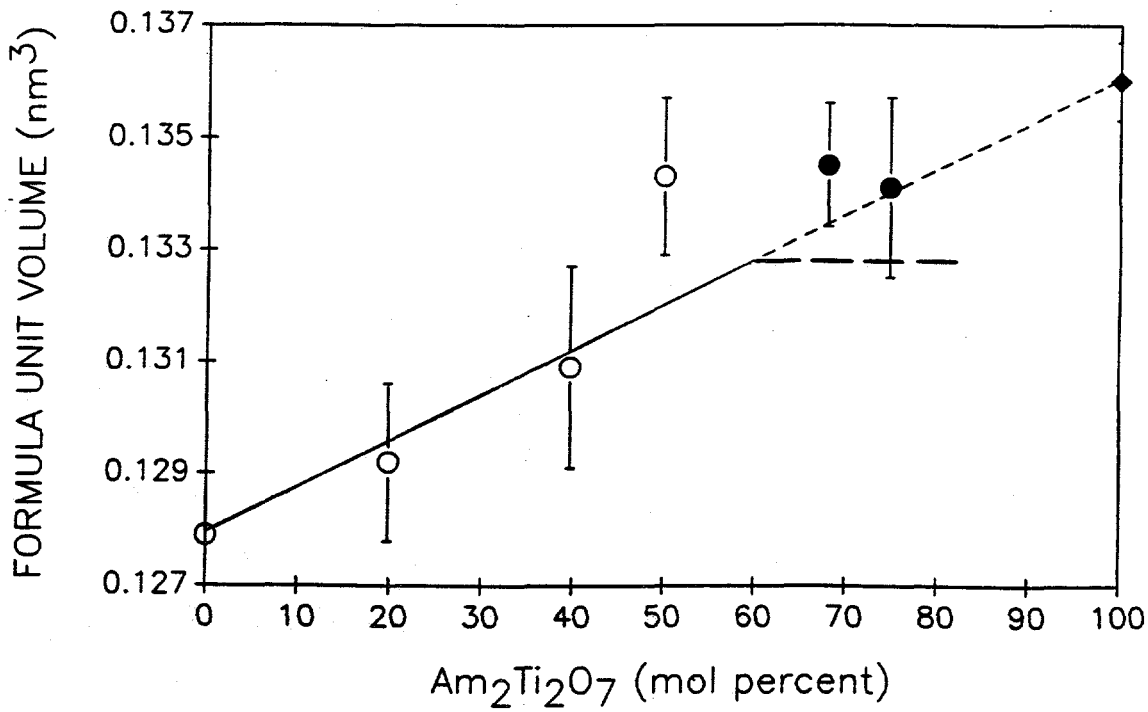

Figure 5. Measured Formula Unit Volume of $Er_{2-x}Am_xTi_2O_7$ versus Mole Percent of $Am_2Ti_2O_7$ in the Initial Mixture. The Sloped Line Connects the Volume of $Er_2Ti_2O_7$ with That of $Am_2Ti_2O_7$ (♦). The Horizontal Line (Filled Symbols) Indicates Saturation of the Host Matrix with $Am_2Ti_2O_7$.

$Am_2Ti_2O_7$ was detected, were calculated from the XRD data. These volumes are plotted as a function of the original mole percent of $Am_2Ti_2O_7$ present in the unfired mixture (Figure 5).

The saturation point for this system is defined as the composition midway between the last preparation yielding only a cubic pyrochlore-type solid solution as detected in the XRD data and the first preparation yielding a cubic pyrochlore-type solid solution and excess monoclinic $Am_2Ti_2O_7$ as detected in the XRD data. The horizontal line drawn through the saturated points is not a least squares line and illustrates the solid solution volumes expected based on this saturation point definition. The volumes of the solid solutions increase with increasing mole percent $Am_2Ti_2O_7$ present in the initial mixture, as expected, until the preparation containing 50 mol percent $Am_2Ti_2O_7$. The volume of the solid solution in this preparation is higher than expected, based on the sloped line connecting the volumes of $Er_2Ti_2O_7$ and $Am_2Ti_2O_7$. Its value is approximately the same as the volumes measured for the saturated solid solutions, but no excess monoclinic $Am_2Ti_2O_7$ was seen in the XRD data from this preparation. The volumes of the saturated solid solutions are quite constant. The solid solubility limit for $Am_2Ti_2O_7$ in $Er_2Ti_2O_7$ (Figure 5) was estimated to be 59±9 mol percent. This limit agrees well with that measured for $Nd_2Ti_2O_7$ (the M(III) ionic radii for Nd and Am are

comparable) in $Er_2Ti_2O_7$ (60.7 mol percent [6]).

D. $Ln_2O_3 \cdot (nTiO_{2-m})$ Solid Solutions (Ln=La, Pr, or Nd) and $Pu_2O_3 \cdot (3TiO_{2-m})$

Perovskite-type compounds $Ln_2O_3 \cdot (nTiO_{2-m})$ (Ln=La-Nd, n=3) with the lanthanide in the III oxidation state and part of the titanium present as Ti(III) are known [7-11]. It has been reported that the value of m is dependent on the conditions in which the compounds are prepared, i.e., the reaction temperature and atmosphere [11]. It has been determined that an additional mole of TiO_{2-m} is soluble in $Ce_2O_3 \cdot (3TiO_{2-m})$ [7] and thus attempts were made to determine the solubility limits of TiO_{2-m} and the value of m in $Ln_2O_3 \cdot (3TiO_{2-m})$ (Ln=La, Pr, or Nd) for compounds synthesized at 1300°C.

The XRD patterns of the lanthanum and neodymium compounds, with n=3.5, matched well with the patterns reported for $Ln_2O_3 \cdot (3TiO_{1.9})$ (Ln=La or Nd) [8]. However when $n \geq 4$, additional phases were observed in the XRD patterns, and these could be identified as Ti_5O_9 and Ti_6O_{11} in the case of Ln=La. The patterns of these titanium suboxides became more intense as the value of n increased. The main XRD pattern from the praseodymium compounds also matched that reported for $Ln_2O_3 \cdot (3TiO_{1.9})$ [8]. However, when n>4, additional phases that could not be identified began to appear in the XRD patterns.

Oxidation in air of single-phase $Ln_2O_3 \cdot (nTiO_{2-m})$ was used to estimate the value of m. Since, as expected, these treatments produced weight gains that resulted from the uptake of oxygen only during the oxidation of Ti(III) to Ti(IV), the weight gain is assumed to be proportional to the oxygen deficiency before oxidation, e.g., a weight gain of 1.48% for $Ln_2O_3 \cdot (3.5TiO_{2-m})$ translates into $m \approx 0.16$ (see Appendix A for example calculation). Thus, the following composition limits were established: $La_2O_3 \cdot (3.5TiO_{1.84})$, $Pr_2O_3 \cdot (4TiO_{1.84})$ and $Nd_2O_3 \cdot (3.5TiO_{1.84})$. These values are in accord with $Ce_2O_3 \cdot (4TiO_{1.89})$ obtained earlier [7].

The synthesis of the plutonium analog of $Ln_2O_3 \cdot (3TiO_{2-m})$ was then attempted. The results of the analysis of the XRD data (Table IV) obtained from the blue-black product indicated that a tetragonally distorted perovskite, with a pattern comparable to that from $Ce_2O_3 \cdot (3TiO_{2-m})$, was formed. The weight gain (2.6%) achieved by air oxidation of $Pu_2O_3 \cdot (3TiO_{2-m})$ was used to estimate the value of $m \approx 0.07$ (see Appendix A for calculation), which is consistent with the formation of PuO_2 and TiO_2. This non-zero value of m confirms the presence of a small amount of Ti(III) and is of the same order of magnitude as the values of m estimated for the light lanthanide analogs [this work and 7]. The lattice parameters calculated for tetragonal $Pu_2O_3 \cdot (3TiO_{1.93})$ are $a_o = 0.384 \pm 0.001$ and $c_o = 0.777 \pm 0.003$ nm and are similar to the parameters of the analogous cerium

Table IV

XRD Data Obtained for

Tetragonal $Pu_2O_3 \cdot (3TiO_{1.93})$

Compared to That for $Ce_2O_3 \cdot (3TiO_{1.89})$

$Pu_2O_3 \cdot (3TiO_{1.93})$			$Ce_2O_3 \cdot (3TiO_{1.89})$	
Int.	d(nm)	hkl	d(nm)	Int.
w	0.764	001	0.795	11
m-	0.387	002,100	0.388	8
w+	0.346	101	0.349	10
s	0.274	110	0.2745	100
vw	0.259	003	0.2602	3
m-	0.223	112	0.2240	25
m	0.194	200	0.1944	19
	0.194	004	0.1939	20
vw	0.186	201	0.1882	8
w	0.173	210		
	0.173	104		
vw	0.167	211		
m+	0.158	212,114	0.1583	31
vw	0.144	213		
w+	0.137	220,204	0.1371	15
w	0.129	006,214	0.1295	3
w+	0.122	310	0.1227	6
	0.122	106	0.1225	6
w	0.117	312,116	0.1171	3
w	0.112	224	0.1119	5
vw	0.107	304	0.1075	2
m-	0.104	320,216	0.1036	9

Measured lattice parameters for tetragonal $Pu_2O_3 \cdot (3TiO_{1.93})$: a_o=0.384±0.001, c_o=0.777±0.003 nm; (film, 114.6 mm Ø, Mo $K_{\bar{\alpha}}$ radiation)
Measured lattice parameters for tetragonal $Ce_2O_3 \cdot (3TiO_{1.89})$: a_o=0.3846±0.0014, c_o=0.7801±0.0037 nm (diffractometer, Cu $K_{\alpha 1}$ radiation)

compound. The volume of the formula unit (2/3 per unit cell based on 2 per unit cell when written $Ln_{2/3}TiO_{3-m}$ [11]) calculated from these parameters is 0.172±0.002 nm^3; it agrees well with the 0.1728 nm^3 determined from the correlation of formula unit volumes of $Ln_2O_3 \cdot (3TiO_{2-m})$ ($m \approx 0.1$) [8 and this work] to ion volumes of Ln(III) [45] (Figure 6).

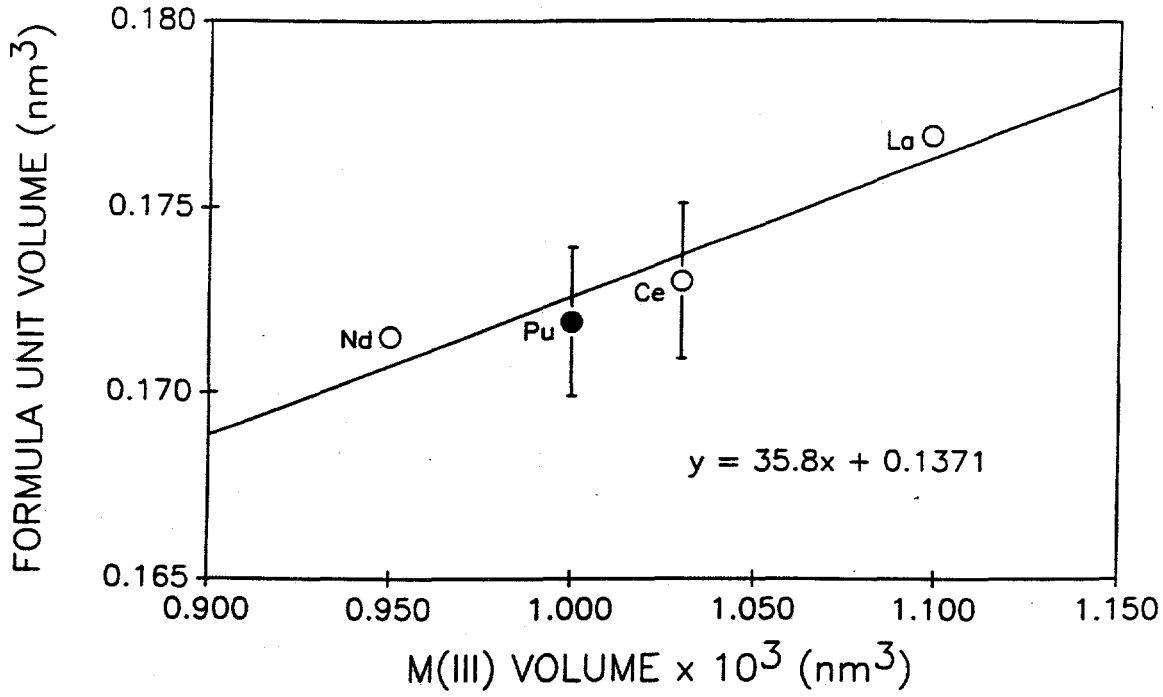

Figure 6. Correlation of Formula Unit Volumes of $Ln_2O_3 \cdot (3TiO_{2-m})$ ($m \approx 0.1$) to Ion Volumes of Ln(III), CN=6 [8,45, and this work]. The Corresponding Plutonium Formula Unit Volume (●) Obtained in This Work Is Included and Is Consistent with This Correlation.

CHAPTER IV

STRONTIUM-CONTAINING PEROVSKITE-TYPE SOLID SOLUTIONS AND COMPOUNDS

A. Background on the $SrO-LnO_{1.5}-TiO_2$ System

Several studies have been performed in the system $SrO-LnO_{1.5}-TiO_2$, much of it with Ln=La, but the findings do not agree. One research group studied the $SrTiO_3-La_2Ti_3O_9$ system and found "cubic perovskite-type solid solutions [14]." When the XRD patterns of some solid solutions, including $SrLa_2Ti_4O_{12}$, showed additional diffraction lines that were twice the d value of lines in the original cubic cell, these solid solutions were concluded to have "multiple-cell cubic perovskite" structures [14]. However, one of the solid solutions which had been quenched at 1400°C did not show these additional lines in the XRD patterns.

Within the $SrO-LaO_{1.5}-TiO_2$ system, a different research group identified a triangular, homogeneous region consisting of cubic perovskite-type solid solutions [15]. They also reported a tetragonal structure for $SrLa_2Ti_4O_{12}$ when it was very slowly cooled from 1300 to 800°C and then quenched [15]. The XRD pattern showed 10 lines in addition to a cubic perovskite-type structure [15], and some of these lines coincided with those reported previously for $SrLa_2Ti_4O_{12}$ [14]. These additional lines were not seen when

the sample was quenched from 1300°C.

A third research group could not confirm the triangular region of cubic perovskite-type homogeneity previously reported but did find three compounds within the $SrO-LaO_{1.5}-TiO_2$ system: $SrLa_2Ti_2O_8$, $SrLa_2Ti_3O_{10}$ and $SrLa_2Ti_4O_{12}$, and the latter was reported to have a tetragonally distorted perovskite-type structure [16].

Compounds of the type $SrLn_4Ti_5O_{17}$ in which Ln=La, Pr, or Nd have also been reported [46]. Based on their studies and the findings of other researchers, one research group concluded that in the $SrO-LnO_{1.5}-TiO_2$ system only $SrLa_4Ti_4O_{15}$, $SrLn_4Ti_5O_{17}$ (Ln=La, Pr, or Nd), and the solid solutions $Sr_{1-y}Ln_{2y/3}TiO_3$ (Ln=La, Pr, or Nd), equivalent to $Sr_{4-x}Ln_{2x/3}Ti_4O_{12}$ used here, form at 1200 to 1300°C [47].

Because of the discrepancies discussed above and because the system had not been studied with cerium, the system $SrO-LnO_{1.5}-TiO_2$ was reinvestigated emphasizing solid solutions in which Ln=Ce or Nd.

B. Formation of Solid Solutions $Sr_{4-x}Ln_{2x/3}Ti_4O_{12}$ (Ln=La-Nd)

A series of solid solutions of composition $Sr_{4-x}Ln_{2x/3}Ti_4O_{12}$ was found to exist along the tie line between $SrTiO_3$ and $Ln_2Ti_3O_9$ (Ln=La, Ce, Pr, or Nd) (Figure 7). Compounds with composition $SrLn_2Ti_4O_{12}$ are selected here as representatives of this series. All conclusions about structures were obtained from analysis of powder XRD data.

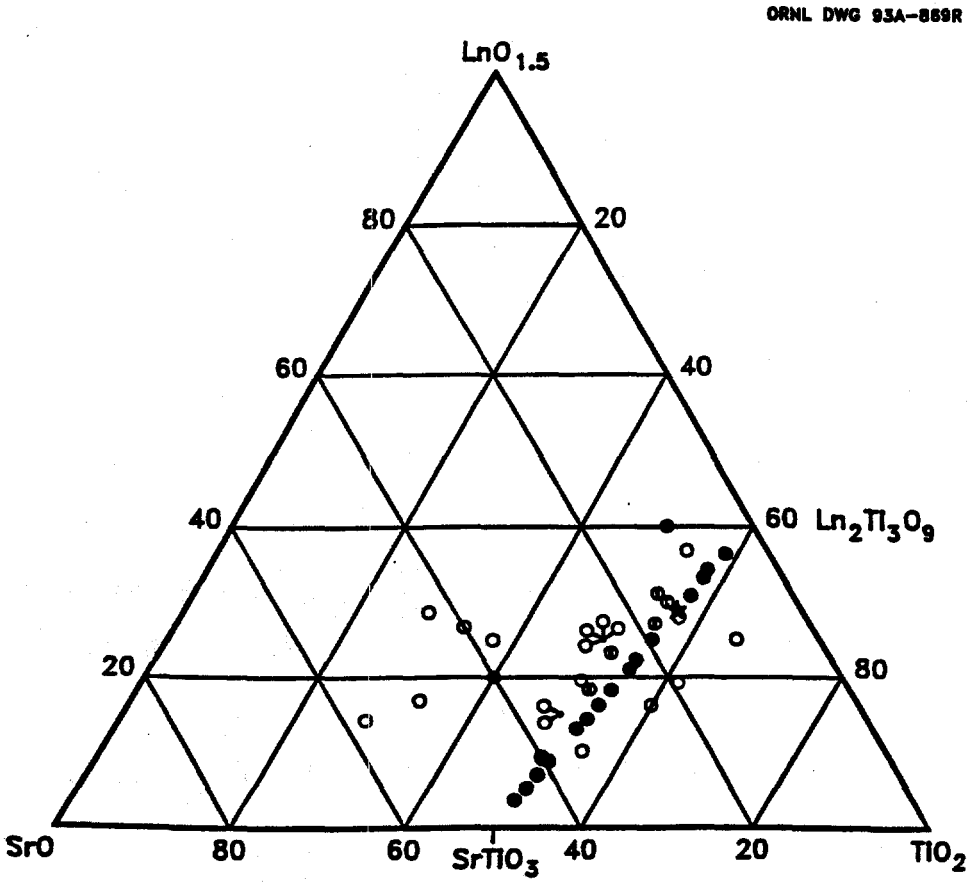

Figure 7. Phase Diagram for $SrO-LnO_{1.5}-TiO_2$ (Ln=La-Nd) at 1400°C.
●: Single Phase; ○: More Than One Phase;
★: $SrLn_2Ti_4O_{12}$
More Than One Symbol, e.g., ⊕ or ⊃, at a Particular Composition Indicates That Several Reactions Were Performed with Different Lanthanides.

While the existence of $SrTiO_3$ having a cubic structure is undisputed, the existence of stoichiometric $Ln_2Ti_3O_9$ on the opposite end of the tie line is questionable. There is agreement that an oxygen deficient $Ln_2Ti_3O_{9-3m}$ exists instead, and several structures (cubic, tetragonal, orthorhombic) have been proposed (see also Chapter III, section D) [8-11]. Under oxidizing conditions, this phase can be stabilized by small amounts of $SrTiO_3$ [22]. Since the structure of $Ln_2Ti_3O_{9-3m}$ will affect the structure of its solid solutions, it is likely that the disagreements in the literature regarding the structure of $Sr_{4-x}Ln_{2x/3}Ti_4O_{12}$ solid solutions [14-16] reflect the disagreements about the structure of $Ln_2Ti_3O_{9-3m}$ [8-11].

The XRD patterns of solid solutions with compositions below 45±5 mol percent $Ln_2Ti_3O_{9-3m}$, see Table V, show a very strong resemblance to that of $SrTiO_3$ [48], with several of the peaks split into two. This splitting of peaks suggests a cubic (distorted slightly to tetragonal) perovskite-type structure [49]. The XRD patterns of solid solutions with compositions above 45±5 mol percent $Ln_2Ti_3O_{9-3m}$, which includes $SrLn_2Ti_4O_{12}$, see Table VI, show a resemblance to those of compositions below 45±5 mol percent $Ln_2Ti_3O_{9-3m}$, in which several of the peaks are split into two, but new peaks are also present. The patterns are similar to those from tetragonal $SrLa_2Ti_4O_{12}$ [15] and also to those from orthorhombic $La_2Ti_3O_{8.979}$ [11]. The tetragonal symmetry was

Table V

XRD Data Obtained for a Tetragonal Solid Solution Containing 81.8 Mol % $SrTiO_3$ and 18.2 Mol % $Ce_2Ti_3O_{9-3m}$

d(nm)	I/I_o	hkl*
0.3926	5	100
0.2753	100	110
0.2248	31	111
0.1952†	27	002
0.1945†	27	200
0.1737	3	210
0.1590	34	211
0.1378	19	220
0.1299	1	300
0.1235†	5	301
0.1231†	12	310
0.1175	6	311
0.1125	6	222
0.1041	10	321
0.09771†	2	004
0.09731†	3	400
0.09193†	3	114
0.09177†	7	411
0.08953	3	331
0.08730†	3	402
0.08706†	5	420

Measured lattice parameters:
a=0.3896±0.0001, c=0.3905±0.0003 nm; (diffractometer, Cu $K_{\alpha 1}$ radiation)

*Indexed on the basis of cubic $SrTiO_3$ (Pm3m) [48] with the additional lines assigned to interplanar spacings arising from a tetragonal distortion [49].
†Indicates lines resulting from the splitting of formerly cubic lines.

Table VI

XRD Data Obtained For a Tetragonal Solid Solution Containing 21.8 Mol % $SrTiO_3$ and 78.2 Mol % $Nd_2Ti_3O_{9-3m}$

d(nm)	I/I_o	hkl*
0.7739	16	001
0.3849	3	002,100
0.3440	12	101
0.2719	100	110
0.2559	8	003
0.2221	37	112
0.1927†	21	004
0.1918†	15	200
0.1876	7	201
0.1727	4	210
0.1677	3	211
0.1573†	34	114
0.1568†	19	212
0.1541	3	203
0.1432	2	213
0.1362†	9	204
0.1360†	12	220
0.1295	3	006
0.1220†	6	106
0.1218†	5	310
0.1213	5	130
0.1163	3	116
0.1112	8	224
0.1030	9	320
0.1028	9	216

Measured lattice parameters:
a=0.3821±0.0011, c=0.7738±0.0030 nm; (diffractometer, Cu $K_{\alpha 1}$ radiation)

*Indexed on the basis of tetragonal $Sm_{0.33}TaO_3$ [50].
†Indicates lines resulting from the splitting of formerly cubic lines.

selected for solid solutions of this composition range because the lines were not split as many times as that seen in orthorhombic $La_2Ti_3O_{8.979}$ [11] and on the basis of other known compounds [50]. It was interesting to observe that although $SrCe_2Ti_4O_{12}$ samples prepared using TiN, in pure argon or a reducing mixture of Ar/4% H_2, have different colors, brown and dark blue, respectively, indicating that the latter had some Ti(III) present, their XRD data were similar with slightly different lattice parameters (mixture fired in Ar: a_o=0.3875±0.0002, c_o=0.7758±0.0005 nm; mixture fired in Ar/4% H_2: a_o=0.3886±0.0001, c_o=0.7760±0.0003 nm).

In addition to the direct synthesis from oxides, members of the neodymium-containing series of solid solutions were also obtained by the reaction:

$$SrNd_2Ti_4O_{12} + nSrTiO_3 \longrightarrow Sr_{1+n}Nd_2Ti_{4+n}O_{12+3n} \qquad (3)$$

$$\downarrow$$

$$\frac{4+n}{4}\left(Sr_{4-\frac{12}{4+n}}Nd_{\frac{24}{12+3n}}Ti_4O_{12}\right)$$

The same results are expected for the lanthanum-, cerium- and praseodymium-containing compounds.

In order to correlate a dimensional property with composition for all the synthesized compounds $Sr_{4-x}Ln_{2x/3}Ti_4O_{12}$ (Ln=La-Nd), formula unit volumes (two per unit cell, number arbitrarily selected since not well-established) were

plotted versus mole percent SrO (Figure 8). The volume increases as the SrO content increases (Figure 8). The data plotted include single phase compositions and compositions which contained monoclinic $Ln_2Ti_2O_7$ in addition to the cubic (slightly distorted to tetragonal) perovskite-type phase. In cases where two known phases were present (as detected by XRD), the composition of the compound $Sr_{4-x}Ln_{2x/3}Ti_4O_{12}$ was empirically estimated by solving a system of simultaneous equations of mass and charge balances (see Appendix B for example calculation), and its SrO content was plotted in Figure 8. Compositions which produced more than two phases, or two phases in which one was unidentified, could not be estimated unequivocally and were omitted from Figure 8. Each line in Figure 8 approaches 50 mol percent SrO and the unit cell volume of $SrTiO_3$. This is to be expected for the condition x=0 in $Sr_{4-x}Ln_{2x/3}Ti_4O_{12}$ ($\approx$ 4 $SrTiO_3$). The volumes of the cerium-containing compounds are larger that those of the corresponding lanthanum compounds instead of smaller, as would be expected based on their ionic radii; this is due to the presence of Ti(III) in the cerium compounds.

C. Reactions of $SrLn_2Ti_4O_{12}$ with SrO

The limits of single phase composition of $Sr_{4-x}Ln_{2x/3}Ti_4O_{12}$ were additionally studied by reaction between $SrLn_2Ti_4O_{12}$ and different amounts of SrO. When 1 mol of SrO was reacted with 1 mol of $SrLn_2Ti_4O_{12}$ for Ln=La, Ce, Pr, or Nd

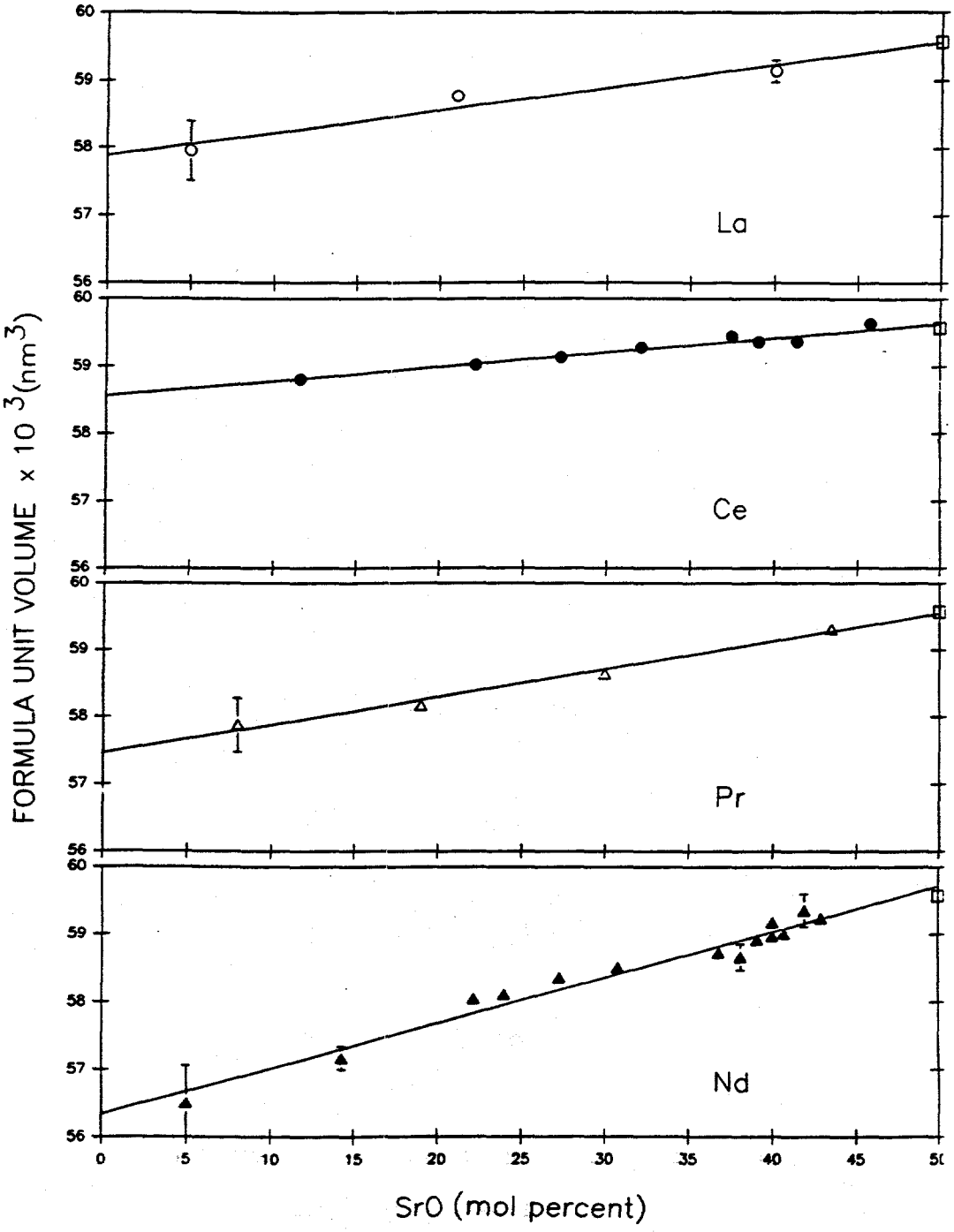

Figure 8. Measured Formula Unit Volume of $Sr_{4-x}Ln_{2x/3}Ti_4O_{12}$ (Ln=La-Nd) versus Mole Percent of SrO.
O: La^{3+}; ●: Ce^{3+}; △: Pr^{3+}; ▲: Nd^{3+}
□: $SrTiO_3$
The Data Points Without Error Bars Have Errors Smaller than the Height of the Symbol.

(Equation (4)), the results indicated that $Ln_2Ti_2O_7$ and a solid solution, with a relatively small value of x ($x \leq 0.5$), i.e., high strontium content, were obtained. This small amount of lanthanide ion was sufficient to distort the structure as indicated by the observed peak splitting. As the amount of SrO was increased, e.g., when 3 mol of SrO were reacted with $SrNd_2Ti_4O_{12}$ (Equation (5)), Nd_2O_3 was found in addition to $SrTiO_3$. When the amount of SrO was increased to 5 (Equation (6)) and then 7 mol (Equation (7)), the products were Nd_2O_3 together with, respectively, $Sr_3Ti_2O_7$ and Sr_2TiO_4.

$$SrLn_2Ti_4O_{12} + SrO \longrightarrow aLn_2Ti_2O_7 + bSr_{4-x}Ln_{2x/3}Ti_4O_{12} \quad (4)$$

$$SrNd_2Ti_4O_{12} + 3SrO \longrightarrow Nd_2O_3 + 4SrTiO_3 \quad (5)$$

$$SrNd_2Ti_4O_{12} + 5SrO \longrightarrow Nd_2O_3 + 2Sr_3Ti_2O_7 \quad (6)$$

$$SrNd_2Ti_4O_{12} + 7SrO \longrightarrow Nd_2O_3 + 4Sr_2TiO_4 \quad (7)$$

D. Comments Regarding Previous Observations in the $SrO-LnO_{1.5}-TiO_2$ System

Under the experimental conditions used, the results obtained and shown in Figure 7 (p. 47) do not confirm the existence of a ternary, single phase, composition area, which is in contrast to that previously reported [15] for

lanthanum compounds. Neither were single phase areas for cerium, praseodymium or neodymium compounds found. Additionally, no apparent effect of the rate of cooling on the structures of the solid solutions was seen, contrary to what was previously reported [14,15].

After identifying the series $Sr_{4-x}Ln_{2x/3}Ti_4O_{12}$ as a stable series of compounds which form in the $SrO-LnO_{1.5}-TiO_2$ system, diffraction patterns obtained from compounds prepared in this work were compared with those of other compounds whose existence had been disputed in the literature. For example, one group [46] concluded that the compound $SrLa_2Ti_3O_{10}$ reported by another group [16] was not a pure compound but a mixture of $SrLa_4Ti_5O_{17}$ and $SrTiO_3$. Results from this work indicate that it consists of a mixture of $Sr_{4-x}La_{2x/3}Ti_4O_{12}$ and $La_2Ti_2O_7$. Attempts to synthesize $SrNd_4Ti_5O_{17}$ revealed that the product was not a pure compound, contrary to previously reported results [46], but a mixture of $Sr_{3.14}Nd_{0.57}Ti_4O_{12}$ and $Nd_2Ti_2O_7$.

E. Formation of $SrAn_2Ti_4O_{12}$ (An=Pu or Am)

It has been determined that smaller ions, such as the heavy trivalent lanthanides and the tetravalent actinides, partition preferentially into the zirconolite phase of SYNROC, the well-studied proposed ceramic waste form [26,51-53]. Larger ions, such as trivalent cerium and neodymium, partition preferentially into the perovskite-type phase

[26,51], as should comparably sized trivalent actinides. Of the two phases, zirconolite has been found to be the more durable in leaching tests [26] and α-decay damage studies [54]. Of the few Pu-containing titanate phases reported before this work, most are zirconolites (e.g., $CaZr_{0.8}Pu_{0.2}Ti_2O_7$ [53], $Ca_{0.8}Pu_{0.2}ZrTi_{1.8}Al_{0.2}O_7$ [53], and $CaPuTi_2O_7$ [55]) except $PuTi_2O_6$, which is similar to brannerite [56]. The oxidation state of plutonium in most of these compounds is IV.

It was expected that Pu(III) would distribute favorably to the perovskite-type phase. Because of the paucity of information on Sr-Pu-Ti-O compounds, titanate compounds containing plutonium and strontium that would form perovskite-type structures were attempted to be synthesized. Such materials would offer the feasibility of immobilizing both actinides and ^{90}Sr.

With the successful formation of perovskite-type $Sr_{4-x}Ln_{2x/3}Ti_4O_{12}$ (Ln=La-Pr) solid solutions, attempts were made to prepare actinide analogs (An=Np-Am) of a representative compound of the series where x=3.0. In the case of plutonium, this was done in accord with the reaction shown in Equation (8) and calcining in Ar/4% H_2. TiN was used as a reductant for plutonium based on earlier success in preparing Ce(III) compounds [7]. The americium analog was prepared by a reaction similar to the one described in Equation (8) but without the use of TiN. Calcination in Ar

at 1300°C was sufficient for the reduction of Am(IV) to Am(III) in this matrix as was also seen for americium in the dititanate compound.

$$SrCO_3 + 2PuO_2 + 0.5TiN + 3.5TiO_2 \longrightarrow SrPu_2Ti_4O_{12} + 0.25N_2 + CO_2 \quad (8)$$

The XRD data for the black $SrPu_2Ti_4O_{12}$ and brick-red $SrAm_2Ti_4O_{12}$ products (Tables VII and VIII) were consistent with those for the comparable, based on ionic radii, light lanthanide compounds, $Sr_{4-x}Ln_{2x/3}Ti_4O_{12}$, having tetragonally distorted perovskite-type structures for values of x larger than 2.84. Line splitting seen with the lanthanide compounds was not observed for the actinide compounds most likely because of the more limited resolution inherent in the film and the shorter wavelength of Mo K_α radiation. The measured tetragonal lattice parameters obtained for the plutonium and americium compounds, respectively, were a_o=0.390±0.001, c_o=0.780±0.001 nm and a_o=0.389±0.001, c_o=0.775±0.002 nm. The formula unit volume (two per unit cell, number arbitrarily selected since not well-established) of the americium compound calculated from these parameters, 0.0586±0.0005 nm^3, is slightly higher than the 0.05730 nm^3 determined from the correlation of formula unit volumes of $SrLn_2Ti_4O_{12}$ (Ln=La, Pr, or Nd) with the ion

Table VII

XRD Data Obtained for

Tetragonal $SrPu_2Ti_4O_{12}$ Compared to That for $SrCe_2Ti_4O_{12}$

$SrPu_2Ti_4O_{12}$			$SrCe_2Ti_4O_{12}$	
Int.	d(nm)	hkl	d(nm)	Int.
		001	0.780	1
m	0.390	002,100	0.388	5
vw	0.351	101	0.347	1
s	0.277	110	0.2744	100
m	0.225	112	0.2240	22
m	0.195	200	0.1945	21
	0.195	004	0.1939	42
		201	0.1881	1
m-	0.174	210,104	0.1735	4
		211	0.1691	1
m+	0.159	212,114	0.1584	42
vw	0.145	213	0.1422	1
m	0.138	220	0.1372	21
	0.138	204	0.1359	1
w	0.130	006,214	0.1293	2
m	0.123	310	0.1230	7
	0.123	106	0.1226	12
w	0.118	312	0.1172	2
	0.118	116	0.1169	5
w	0.113	224	0.1120	6
vw	0.108	304	0.1076	1

Measured lattice parameters for tetragonal $SrPu_2Ti_4O_{12}$: a_o=0.390±0.001, c_o=0.780±0.001 nm; (film, 114.6 mm Ø, Mo $K_{\bar{\alpha}}$ radiation)
Measured lattice parameters for tetragonal $SrCe_2Ti_4O_{12}$: a_o=0.3886±0.0001, c_o=0.7760±0.0003 nm; (diffractometer, Cu $K_{\alpha 1}$ radiation)

Table VIII

XRD Data Obtained for

Tetragonal $SrAm_2Ti_4O_{12}$ Compared to That for $SrNd_2Ti_4O_{12}$

$SrAm_2Ti_4O_{12}$			$SrNd_2Ti_4O_{12}$	
Int.	d(nm)	hkl	d(nm)	Int.
m-	0.387	002,100	0.384	4
		101	0.348	1
s	0.273	110	0.2722	100
m-	0.226	112	0.2224	24
m-	0.195	004	0.1926	31
	0.195	200	0.1915	2
		201	0.1876	2
w+	0.173	210,104	0.1727	4
m	0.158	212,114	0.1574	36
vw	0.143	213		
w-	0.139	220,204	0.1363	23
vw	0.129	006,214	0.1284	2
w	0.123	310,106	0.1220	7
w+	0.118	312	0.1178	1
	0.118	116	0.1163	3
vw	0.112	224	0.1114	5

Measured lattice parameters for tetragonal $SrAm_2Ti_4O_{12}$: a_o=0.389±0.001, c_o=0.775±0.002 nm; (film, 114.6 mm Ø, Mo K_α radiation)
Measured lattice parameters for tetragonal $SrNd_2Ti_4O_{12}$: a_o=0.3866±0.0006, c_o=0.7708±0.0014 nm; (diffractometer, Cu $K_{\alpha 1}$ radiation)

volumes of Ln(III) (Figure 9). The measured formula unit cell volume of $SrPu_2Ti_4O_{12}$, 0.0593±0.0004 nm^3, is higher than the value predicted from Figure 9, 0.05785 nm^3, most likely due to the presence of some Ti(III).

Neptunium did not form this perovskite-type compound following the reaction in Equation (8), p. 57. Instead, the XRD data indicated that $SrTiO_3$, NpO_2, and Ti_3O_5 were the products present. It was thought that the temperature at which the NpO_2 had been prepared was perhaps too high, rendering the NpO_2 unreactive under the experimental conditions used here. Therefore, an attempt was made to form $SrNp_2Ti_4O_{12}$ using a different source of NpO_2 prepared at a lower temperature. Likewise, the compound did not form, and the products identified were the same ones as when the "high-fired" NpO_2 was used. This appears to be indicative of the redox behavior of neptunium in these titanate systems, because a similar behavior was seen for the unsuccessful synthesis attempt of $Np_2Ti_2O_7$.

F. Attempts to Prepare $Sr_2An_2Ti_5O_{16}$ (An=Np-Am) and $Sr_2Ce_{2-y}An_yTi_5O_{16}$ (An=Np or Pu)

While no Np(III) analog of $SrLn_2Ti_4O_{12}$ was obtained, it was expected that compounds such as $Sr_{6-12x}Ce_{6x}Ti_5O_{16}$ [17] might stabilize An(IV). This series of compounds is perovskite-like with very similar XRD patterns and lattice parameters as the series $Sr_{4-x}Ln_{2x/3}Ti_4O_{12}$ where $x<2.84$ (cubic slightly

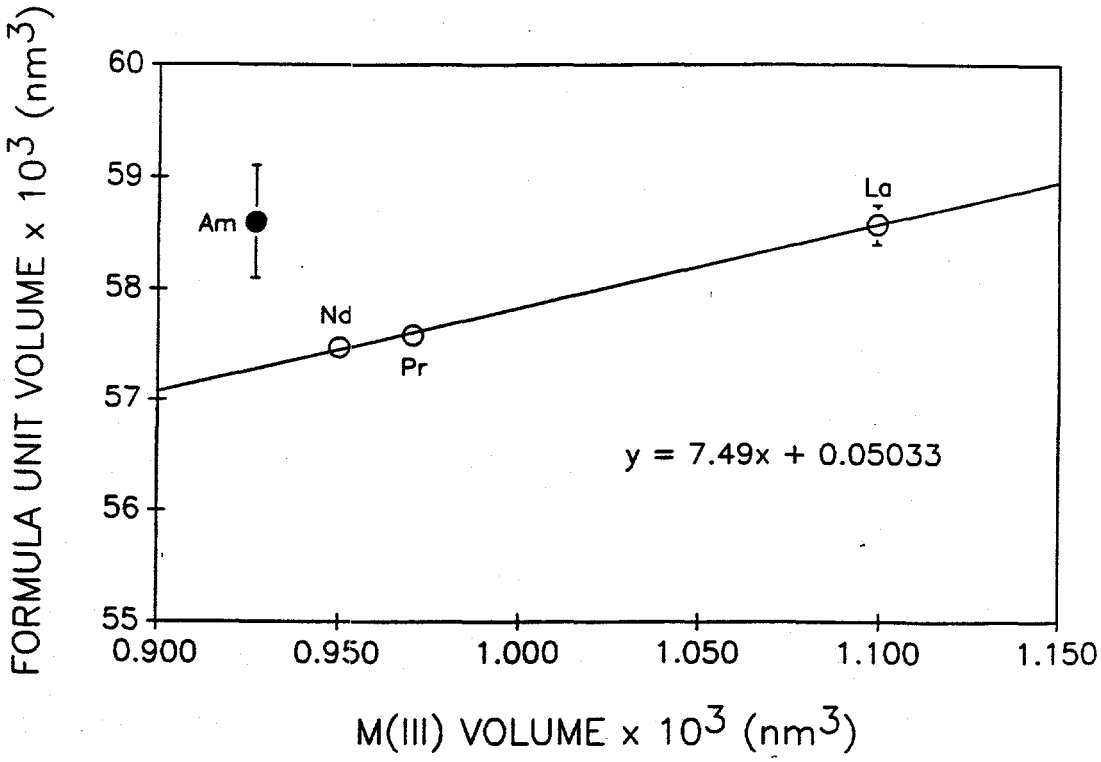

Figure 9. Correlation of Formula Unit Volumes of $SrLn_2Ti_4O_{12}$ to Ion Volumes of Ln(III), CN=6. The Data Points Without Error Bars Have Errors Smaller than the Height of the Symbol. The Corresponding Americium Formula Unit Volume (●) Obtained in This Work Is Included.

distorted to tetragonal). Thus, attempts were made to prepare the An(IV) (An=Np-Am) analogs of $Sr_2Ce_2Ti_5O_{16}$, a member of the series $Sr_{6-12x}Ce_{6x}Ti_5O_{16}$ where $x \approx 0.33$.

Although up to three different routes of preparation were tried for synthesizing $Sr_2An_2Ti_5O_{16}$ (Equations (9-11)), none of them resulted in the desired single-phase product.

$$2SrO + 2AnO_2 + 5TiO_2 \text{ (air)} \quad (9)$$

$$2SrO + An_2Ti_2O_7 + 3TiO_2 \text{ (air)} \quad (10)$$

$$SrPu_2Ti_4O_{12} + SrTiO_3 \quad (11)$$
$$\text{(first Ar/4\% } H_2\text{, then air)}$$

$$\Big\} \not\longrightarrow \quad Sr_2An_2Ti_5O_{16}$$

In attempting to prepare $Sr_2Np_2Ti_5O_{16}$, following the reaction described by Equation (9), the products that resulted were NpO_2, the metastable $NpTi_2O_6$, and $SrTiO_3$. In the case of plutonium, all of the attempts resulted in $SrTiO_3$ and unreacted PuO_2 and TiO_2 as seen from the XRD data. After the first attempt, it was speculated that the PuO_2 used may have been unreactive in air; therefore, $Pu_2Ti_2O_7$ was used as a reactant. Also, $SrPu_2Ti_4O_{12}$ and $SrTiO_3$ were fired together, initially in Ar/4% H_2 and then in air to promote the formation of a Pu(III)-containing single phase [$1.25(Sr_{1.6}Pu_{1.6}Ti_4O_{12})$] observed to occur with the neodymium analog. The subsequent oxidation of this phase was expected

to convert the Pu(III) to Pu(IV) without decomposing the resulting compound into components. As indicated in Equation (11), this approach did not succeed.

The reaction described in Equation (10) was followed in an attempt to prepare $Sr_2Am_2Ti_5O_{16}$. Because of the lack of thermal stability of Am(IV) in the titanate systems studied thus far (and the previous results seen for neptunium and plutonium), it was not considered likely that the compound would form. The XRD data indicated that a perovskite-type compound did form, although there were two very weak, additional lines that could not be indexed on the basis of the perovskite system and could not be matched to any compound in the system. If Am(III) were stable in air at 1250°C in the titanate matrix, the compound could be an actinide analog of a solid solution from the series $Sr_{4-x}Ln_{2x/3}Ti_4O_{12}$. This possible scenario can be described by the reaction in Equation (12).

$$2SrO + Am_2Ti_2O_7 + 3TiO_2 \text{ --> } 1.25(Sr_{1.6}Am_{1.6}Ti_4O_{12}) \qquad (12)$$

A similar reaction using different reactants but the same overall stoichiometry was performed with neodymium (see Equation (3), n=1, p. 51) and yielded a cubic (slightly distorted to tetragonal) perovskite-type compound. Unfortunately, the lattice parameters of the compounds from the $Sr_{6-12x}Ce_{6x}Ti_5O_{16}$ and $Sr_{4-x}Ln_{2x/3}Ti_4O_{12}$ series are very similar,

making unambiguous identification of the perovskite-type compound present difficult.

After the unsuccessful preparation of pure An analogs of $Sr_2Ce_2Ti_5O_{16}$ for neptunium, plutonium, and most likely americium, it was thought that it might be possible to replace part of the Ce(IV) with An(IV). This led to attempts to prepare solid solutions having the compositions $Sr_2Ce_{0.98}Np_{1.02}Ti_5O_{16}$, $Sr_2Ce_{1.41}Np_{0.59}Ti_5O_{16}$, $Sr_2Ce_{1.01}Pu_{0.99}Ti_5O_{16}$ and $Sr_2Ce_{1.60}Pu_{0.40}Ti_5O_{16}$. However, the XRD results indicated that the solid solutions did not form, but instead AnO_2, TiO_2, and a cubic phase were present. The latter is a mixture of $SrTiO_3$ and $Sr_2Ce_2Ti_5O_{16}$, but the two have very similar lattice parameters and are thus not likely resolved on the film.

The inability to prepare $Sr_2An_2Ti_5O_{16}$ and the solid solutions in $Sr_2Ce_2Ti_5O_{16}$ was unexpected. The size of the ions is usually considered a major factor when determining whether a compound will form with perovskite-type symmetry [57]. For example, regarding the synthesized $Sr_2Ce_2Ti_5O_{16}$ and the theoretical $Sr_2Pu_2Ti_5O_{16}$, there is virtually no difference in the ionic radii of Ce(IV) and Pu(IV) [45]. Therefore, the inability to form $Sr_2Pu_2Ti_5O_{16}$ cannot be attributed to size difference. Other factors such as polarizability, charge, and electronic configuration of the ions also contribute to the formation of a compound. In this case, charge cannot be the determining factor as both cerium and plutonium are in the IV oxidation state. Polarizability

seems not to be the determining factor either. Even if plutonium is more polarizable than cerium in every common oxidation state, this did not inhibit the formation of a plutonium analog of $SrCe_2Ti_4O_{12}$, which is a distorted perovskite. When comparing electron configurations, there are no f electrons in Ce(IV) while Pu(IV) has a $5f^4$ electronic configuration. Perhaps the presence of the f electrons somehow interferes with the formation of $Sr_2Pu_2Ti_5O_{16}$. However, both Ce(III) and Pu(III) have f electrons, and the formation of $SrCe_2Ti_4O_{12}$ and $SrPu_2Ti_4O_{12}$ was not inhibited. Other properties that were considered, such as free energies of formation and crystal lattice energies, did not suggest any trends or significant differences that would explain the experimental results. It has been suggested that having more information on the crystal systems might show small, but significant, differences in these crystal lattice energies compared to values calculated using the current information known [58]. Similar arguments can be made for neptunium and americium. At this time, there is no adequate explanation for the inability to synthesize $Sr_2An_2Ti_5O_{16}$.

CHAPTER V

TITANIUM- AND ZIRCONIUM-CONTAINING PYROCHLORE- AND PEROVSKITE-TYPE COMPOUNDS

A. Background

The lanthanide dititanates, $Ln_2Ti_2O_7$, from lanthanum to neodymium, are of monoclinic symmetry [2], while the dititanates, $Ln'_2Ti_2O_7$, from samarium to lutetium exhibit the cubic pyrochlore-type structure [5]. Similarly to the lanthanide dititanates, the lanthanide dizirconates do not all exhibit the same crystal structure. The lanthanide dizirconates, $Ln_2Zr_2O_7$, from lanthanum to gadolinium adopt the cubic pyrochlore-type structure [5], while the remaining lanthanide dizirconates, $Ln'_2Zr_2O_7$, exhibit a defect fluorite structure [5].

The existence of complex pyrochlores has been well established, and there are many examples of such lanthanide-containing compounds in the literature [59]. However, few cases are known of mixed titanium-zirconium pyrochlores. The solubility of $Gd_2Ti_2O_7$ in $Gd_2Zr_2O_7$ has been examined, and complete miscibility of the pyrochlore-type dititanate in the pyrochlore-type dizirconate has been observed [19]. A series of solid solutions $Y_2(Zr_nTi_{1-n})_2O_7$ was reported to exist where the structure of the solid solutions changed from pyrochlore-type to defect fluorite with increasing

zirconium content [20]. However, small amounts of a fluorite-like phase, increasing with zirconium content, were determined to be present along with the solid solution at all compositions [20].

Likewise, there are few known cases of mixed titanium-zirconium compounds or solid solutions exhibiting perovskite-type structures. The system $Na_{0.5}La_{0.5}Ti_{1-x}Zr_xO_3$, which written to follow the notation used in this work would be equivalent to $Na_2La_2Ti_{4-y}Zr_yO_{12}$ where y=4x, was investigated, and perovskite-type solid solution formation at any composition has been reported [21].

In order to augment our knowledge on the existence of pyrochlore-pyrochlore-type solid solutions containing titanium and zirconium, the systems $Nd_2Zr_2O_7$-$Er_2Ti_2O_7$ and $Nd_2Zr_2O_7$-$Nd_{1.2}Er_{0.8}Ti_2O_7$ were studied. There are no known examples of solid solutions resulting from monoclinic dititanates and defect fluorite or pyrochlore-type dizirconates. Therefore, the solubility of $Nd_2Ti_2O_7$, which exhibits monoclinic structure, in defect fluorite $Er_2Zr_2O_7$ was determined. Also the solubility of monoclinic dititanates, $Ce_2Ti_2O_7$ and $Nd_2Ti_2O_7$, in a dizirconate, having pyrochlore-type symmetry and containing the same lanthanide, was examined. The systems $Nd_2Zr_2O_7$-TiO_2 and $Nd_2Ti_2O_7$-ZrO_2 were examined to ascertain pyrochlore-type solid solution formation and to define a region of solid solubility in the $NdO_{1.5}$-TiO_2-ZrO_2 ternary system. Also, attempts were made to

replace some of the titanium by zirconium in the perovskite-type compounds $SrNd_2Ti_4O_{12}$ and $Sr_2Ce_2Ti_5O_{16}$.

It appeared that equilibrium was harder to reach in these systems than in the titanium only systems; much longer reaction times, higher temperatures, and many regrindings were necessary. This may be caused by the inert behavior of ZrO_2 during solid-solid reactions.

B. Pyrochlore-Type Solid Solution Formation in the Systems $Nd_2Zr_2O_7$-$Er_2Ti_2O_7$ and $Nd_2Zr_2O_7$-$Nd_{1.2}Er_{0.8}Ti_2O_7$

In the system $Nd_2Zr_2O_7$-$Er_2Ti_2O_7$, where both compounds exhibit cubic pyrochlore-type structures, complex cubic pyrochlore-type solid solutions, which have the composition $(Nd_{2-x}Er_x)(Ti_xZr_{2-x})O_7 \approx [1\text{-}0.5x\ Nd_2Zr_2O_7 \cdot 0.5x\ Er_2Ti_2O_7]$, were found to form at any value of x. A plot of formula unit volume (eight per unit cell) of the solid solution <u>versus</u> mole percent $Er_2Ti_2O_7$ in the mixture shows a linear correlation that obeys Vegard's Law (Figure 10).

Another system, $Nd_2Zr_2O_7$-$Nd_{1.2}Er_{0.8}Ti_2O_7$, was also examined for solid solution formation because $Nd_{1.2}Er_{0.8}Ti_2O_7$ is a pyrochlore-type solid solution between $Nd_2Ti_2O_7$ and $Er_2Ti_2O_7$ (see Chapter III, section A). It was found that even this complex pyrochlore-type dititanate was miscible with the pyrochlore-type $Nd_2Zr_2O_7$ forming complex pyrochlore-type solid solutions which have the composition $(Nd_{2-x}Er_x)(Ti_{2.5x}Zr_{2-2.5x})O_7 \approx [1.25x\ Nd_{1.2}Er_{0.8}Ti_2O_7 \cdot$

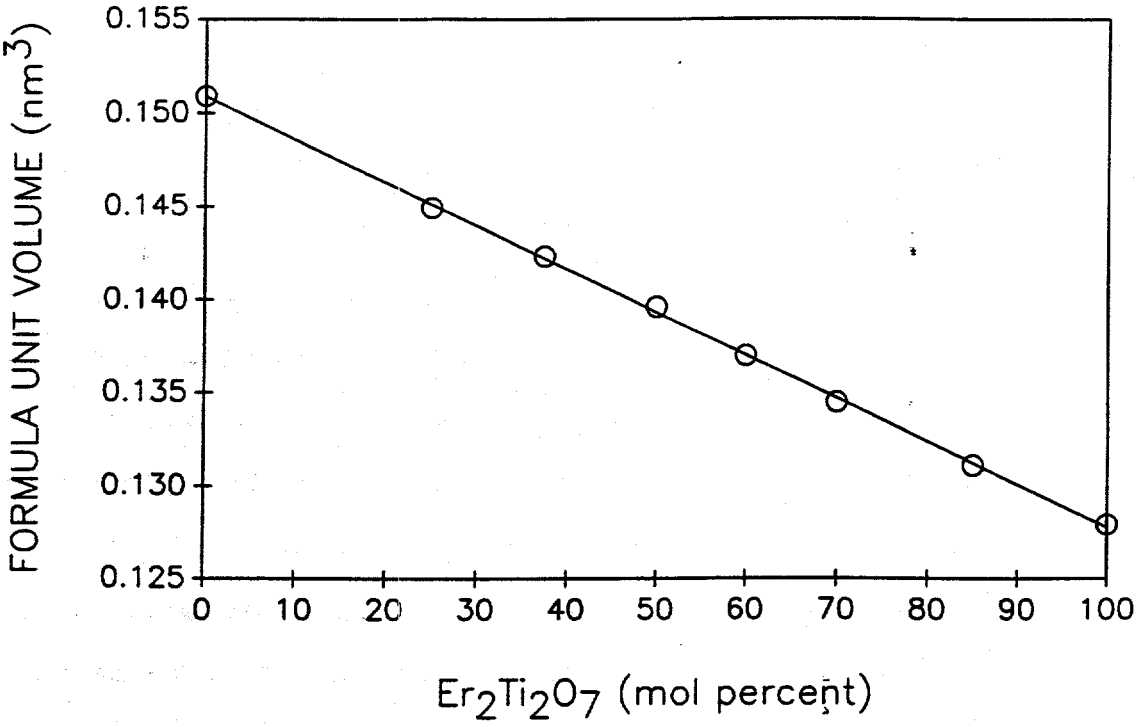

Figure 10. Measured Formula Unit Volume of $(Nd_{2-x}Er_x)(Ti_xZr_{2-x})O_7$ versus Mole Percent of $Er_2Ti_2O_7$ in the Initial Mixture. The Errors for the Data Points Are Smaller than the Height of the Symbols.

1-1.25x $Nd_2Zr_2O_7$]. The measured formula unit volumes (eight per unit cell) of the solid solutions decrease linearly with increasing mole percent of the smaller $Nd_{1.2}Er_{0.8}Ti_2O_7$ in the mixture (Figure 11).

C. Pyrochlore-Type Solid Solution Formation in the System $Nd_2Ti_2O_7$-$Er_2Zr_2O_7$

The system $Nd_2Ti_2O_7$-$Er_2Zr_2O_7$ is the reciprocal of the system $Nd_2Zr_2O_7$-$Er_2Ti_2O_7$ discussed above; however, $Nd_2Ti_2O_7$ exhibits monoclinic symmetry while $Er_2Zr_2O_7$ exhibits defect fluorite structure. Some solubility of $Nd_2Ti_2O_7$ in $Er_2Zr_2O_7$ has been observed. The XRD analysis of preparations containing up to 75 mol percent $Nd_2Ti_2O_7$ indicated that they consisted of pyrochlore-type solid solutions. As shown in Figure 12, the formula unit volume (eight per unit cell) of the solid solution decreases with increasing mole percent of $Nd_2Ti_2O_7$, but with a slope that is not consistent with the slope expected if Vegard's Law were obeyed. This behavior would suggest that the components of the system are not mutually soluble and that at some composition the pyrochlore-type solid solution formed becomes saturated. The additional phase most likely expected after saturation has been reached would be $Nd_2Ti_2O_7$, but only the pyrochlore-type phase was detected from the XRD data from any of the preparations. If $Nd_2Ti_2O_7$ were present, it would be difficult to see at very low concentrations because the most

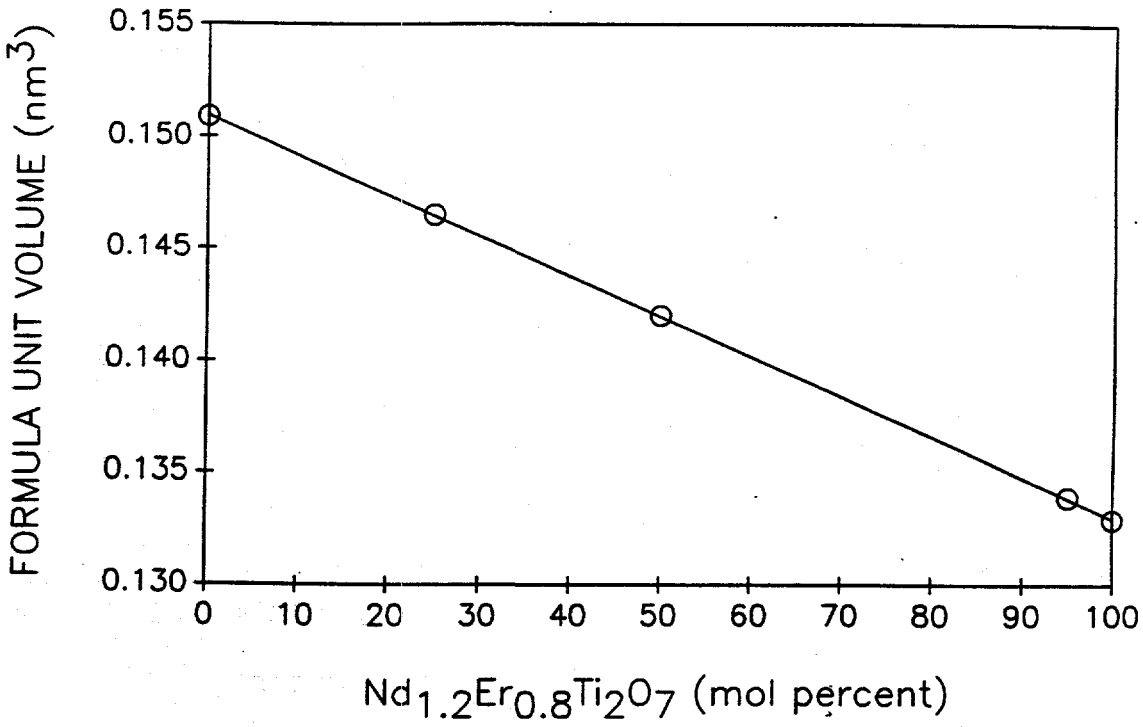

Figure 11. Measured Formula Unit Volume of $(Nd_{2-x}Er_x)(Ti_{2.5x}Zr_{2-2.5x})O_7$ versus Mole Percent of $Nd_{1.2}Er_{0.8}Ti_2O_7$ in the Initial Mixture. The Errors for the Data Points Are Smaller than the Height of the Symbols.

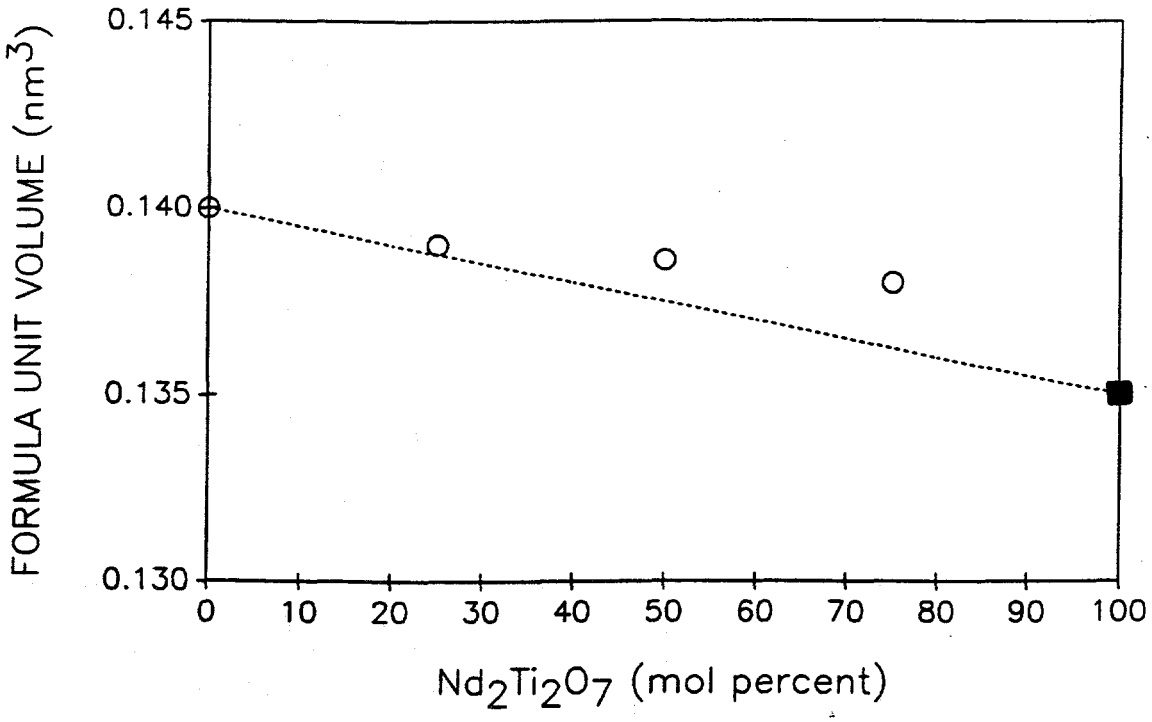

Figure 12. Measured Formula Unit Volume of the Pyrochlore-Type Solid Solution between $Nd_2Ti_2O_7$ and $Er_2Zr_2O_7$ versus Mole Percent of $Nd_2Ti_2O_7$ (■) in the Initial Mixture. The Dotted Line Represents the Line Expected if Vegard's Law Is Obeyed. The Errors for the Data Points Are Smaller than the Height of the Symbols.

intense diffraction line of $Nd_2Ti_2O_7$ would be almost coincident with the most intense line belonging to the solid solution.

D. Pyrochlore-Type Solid Solution Formation in the Systems $Ce_2Ti_2O_7$-$Ce_2Zr_2O_7$ and $Nd_2Ti_2O_7$-$Nd_2Zr_2O_7$

Attempts to form pyrochlore-type solid solutions of the type $Ce_2Zr_{2-x}Ti_xO_7$ between $Ce_2Zr_2O_7$ and $Ce_2Ti_2O_7$ ≈ [1-0.5x $Ce_2Zr_2O_7$ · 0.5x $Ce_2Ti_2O_7$] were unsuccessful. One problem was that under the experimental conditions used, it was difficult to maintain the cerium as Ce(III) and the titanium as Ti(IV) while allowing sufficient reaction time for equilibrium to be reached.

The compound $Ce_2Zr_2O_7$ has been previously reported as prepared in the system $BaCl_2$-$CeCl_3$-$BaZrO_3$ [60]. In the present work, it was prepared following the reaction in Equation (13). ZrN was used to reduce Ce(IV) to Ce(III) similarly to the use of TiN earlier (see Chapter III, section A).

$$2CeO_2 + 0.5ZrN + 1.5ZrO_2 \text{ ---> } Ce_2Zr_2O_7 \qquad (13)$$

A mixture calcined at 1450°C for a total of 40 hours in Ar/4% H_2 yielded a cubic pyrochlore-type with XRD data matching that found in the literature for $Ce_2Zr_2O_7$ [60]. However, calcining this pyrochlore-type compound in Ar at

1350°C for 30 additional hours caused a structural change from the ordered pyrochlore to a disordered defect fluorite structure. This structural change is most likely due to the presence of small amounts of Ce(IV) formed from Ce(III) via oxidation by traces of oxygen inherently present in the argon used. This tentative conclusion is based on the knowledge that the ionic radius of Ce(IV) is similar to that of the heavier lanthanides, Ln'(III) [45], which form defect fluorite dizirconates.

A similar behavior was exhibited by the composition $Ce_2Zr_{1.9}Ti_{0.1}O_7$ as indicated by the results of the following preparations. Calcining in Ar/4% H_2 yielded a pyrochlore-type compound, but unreacted ZrO_2 was also detected from the XRD data. Short calcination times in Ar at 1200°C resulted in incomplete reaction while additional calcination at 1350°C eventually resulted in the formation of a defect fluorite compound due to the possible presence of Ce(IV).

As the titanium content was increased, preparations calcined in Ar/4% H_2 at 1450°C yielded multiple products including a phase similar to the perovskite-type $Ce_2O_3 \cdot (3TiO_{2-m})$, which indicated that reduction of the titanium had taken place. The calcination of one of these preparations in Ar resulted in the formation of $Ce_2Ti_2O_7$ and at least one additional minor cubic phase. Identifying the phase as a pyrochlore-type or a fluorite was not possible without ambiguity because of the presence of numerous, more

intense lines resulting from $Ce_2Ti_2O_7$.

It was possible to prepare, by calcining in Ar/4% H_2, a solid solution of composition $Er_{1.78}Ce_{0.22}Ti_{0.5}Zr_{1.5}O_7$ which exhibited a defect fluorite structure similar to that observed for $Er_2Zr_2O_7$. This solid solution was prepared for use in solubility tests to determine the influence of zirconium on the aqueous solubility of this solid solution compared to that of $Er_{1.78}Ce_{0.22}Ti_2O_7$.

Regarding the system $Nd_2Ti_2O_7$-$Nd_2Zr_2O_7$, it was determined that there is some solubility of $Nd_2Ti_2O_7$ in $Nd_2Zr_2O_7$. Cubic pyrochlore-type solid solutions which have the composition $Nd_2Zr_{2-x}Ti_xO_7 \approx [0.5x\ Nd_2Ti_2O_7 \cdot 1\text{-}0.5x\ Nd_2Zr_2O_7]$ were found to exist up to an x value of approximately 0.86. A plot of formula unit volumes (eight per unit cell) of the solid solutions <u>versus</u> mole percent $Nd_2Ti_2O_7$ in the solid solution indicates that the former decreases with an increase in $Nd_2Ti_2O_7$ concentration up to the point of saturation (Figure 13). At this point, defined by the intersection of the sloped and horizontal lines in Figure 13, the volume of the solid solution remains fairly constant and $Nd_2Ti_2O_7$, in addition to the cubic solid solution, is detected in the XRD data. The XRD patterns of preparations of overall composition $Nd_2Zr_2O_7$, Nd_2ZrTiO_7, $Nd_2Zr_{0.5}Ti_{1.5}O_7$, and $Nd_2Ti_2O_7$, used to detect excess $Nd_2Ti_2O_7$ when past the saturation point, are shown in Figure 14. It can be seen that a slight amount of $Nd_2Ti_2O_7$ is present, in addition to the cubic

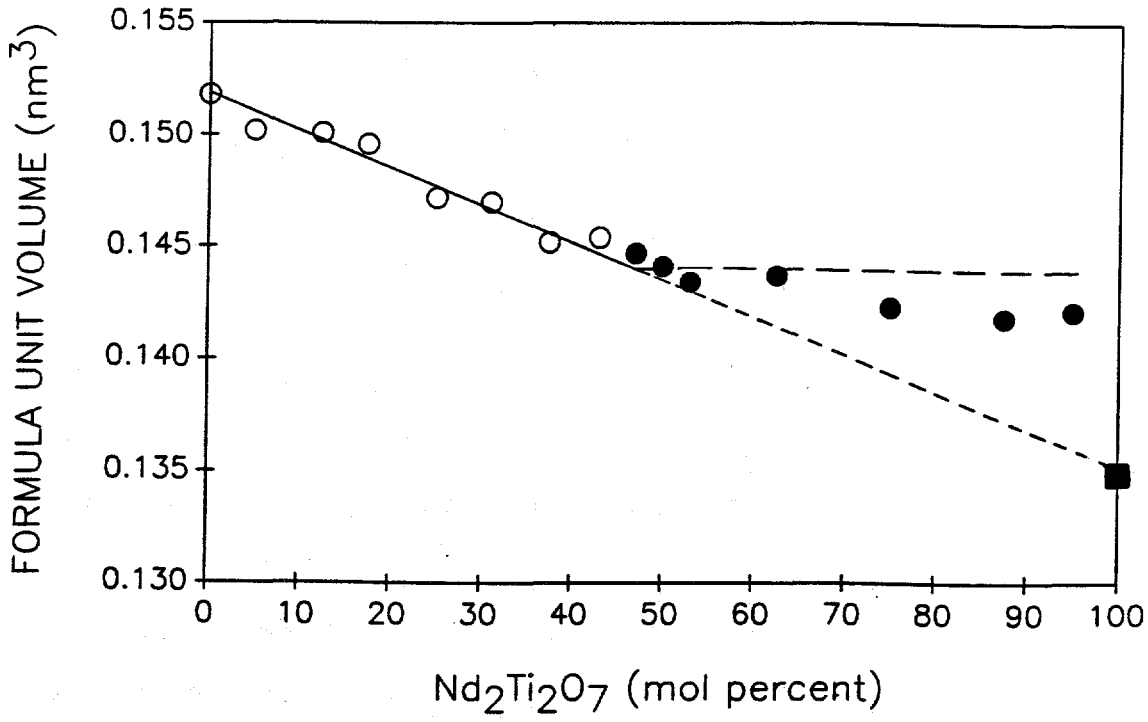

Figure 13. Measured Formula Unit Volume of $Nd_2Zr_{2-x}Ti_xO_7$ versus Mole Percent of $Nd_2Ti_2O_7$ in the Initial Mixture. The Sloped Line Connects the Volume of $Nd_2Zr_2O_7$ with That of $Nd_2Ti_2O_7$ (■). The Horizontal Line (Filled Symbols) Indicates Saturation of the Host Matrix with $Nd_2Ti_2O_7$. The Errors for the Data Points Are Smaller than the Height of the Symbols.

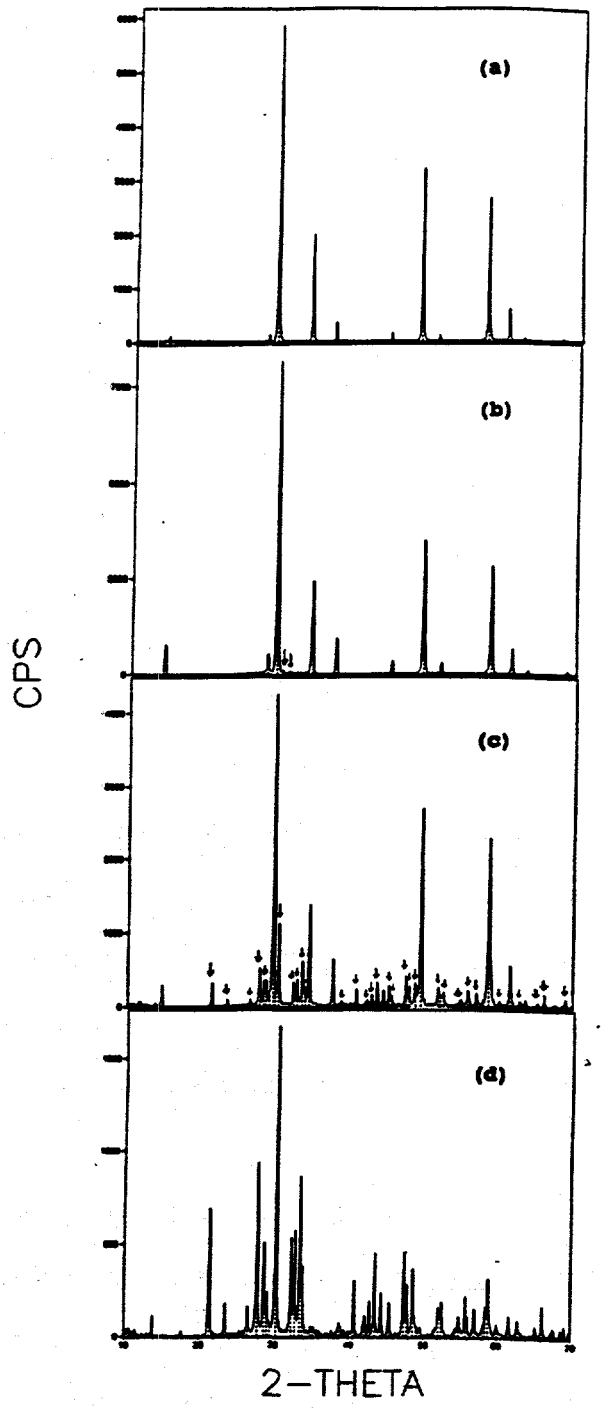

Figure 14. XRD Patterns of Preparations of Overall Composition (a) $Nd_2Zr_2O_7$, (b) Nd_2ZrTiO_7, (c) $Nd_2Zr_{0.5}Ti_{1.5}O_7$, and (d) $Nd_2Ti_2O_7$. ↓Indicates Presence of $Nd_2Ti_2O_7$ in Preparations (b) and (c).

pyrochlore-type solid solution, in the pattern from the preparation with an overall composition of Nd_2ZrTiO_7. The presence of $Nd_2Ti_2O_7$ is even more obvious in the pattern from the preparation of overall composition $Nd_2Zr_{0.5}Ti_{1.5}O_7$.

E. Pyrochlore-Type Solid Solution Formation in the Systems $Nd_2Zr_2O_7$-TiO_2 and $Nd_2Ti_2O_7$-ZrO_2

In the system $Nd_2Zr_2O_7$-TiO_2, it was found that up to approximately 0.56 mol of TiO_2 was soluble in 1 mol $Nd_2Zr_2O_7$ forming a cubic pyrochlore-type solid solution. Additional amounts of TiO_2, up to approximately 1.5 mol, were incorporated into a pyrochlore-type solid solution, but ZrO_2 was displaced. When 2 mol of TiO_2 were reacted, the phase $Zr_{1-x}Ti_xO_2$ separated. When 2.5 mol of TiO_2 were reacted with $Nd_2Zr_2O_7$, the system was severely disrupted, and the XRD data from the preparation indicated the presence of $Nd_2Ti_2O_7$, $Zr_{1-x}Ti_xO_2$, and a pyrochlore with a volume close to that of pure $Nd_2Zr_2O_7$.

A plot of formula unit volume (eight per unit cell) of the solid solution <u>versus</u> the number of moles of TiO_2 reacted per mole $Nd_2Zr_2O_7$ (Figure 15) illustrates the decrease in the volume with increasing amount of TiO_2. However, the decrease is not linear over the entire range of TiO_2 studied; there appear to be three different regions of linearity (A, B, and C denoted in Figure 15) depending on the composition of the solid solution. The slope of the

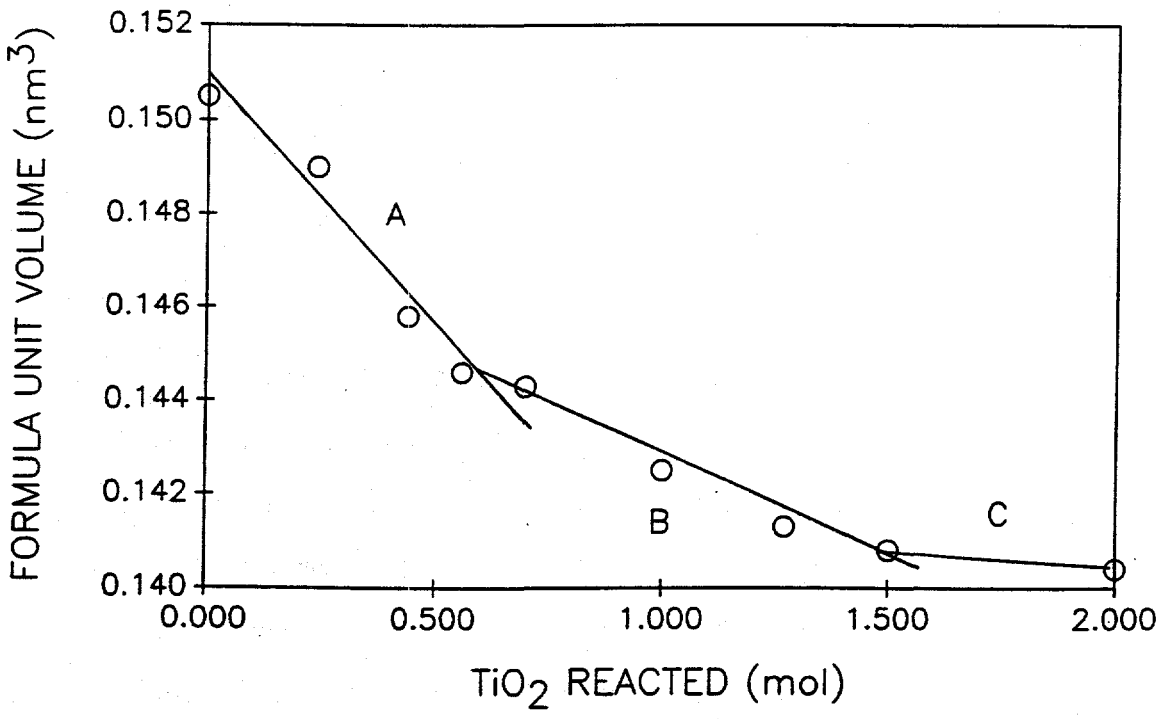

Figure 15. Measured Formula Unit Volume of Pyrochlore-Type Solid Solution between $Nd_2Zr_2O_7$ and TiO_2 versus the Number of Moles of TiO_2 Reacted per Mole of $Nd_2Zr_2O_7$. A, B, and C Denote Three Different Regions of Linearity. The Errors for the Data Points Are Smaller Than the Height of the Symbols.

line resulting from preparations producing single-phase pyrochlore-type solid solutions is steep (Line A) with the concentrations of neodymium, titanium, and zirconium changing for each solid solution; examples are given in Equations (14) and (15).

$$Nd_2Zr_2O_7 + 0.24TiO_2 \longrightarrow 1.07Nd_{1.87}Ti_{0.22}Zr_{1.87}O_7 \quad (14)$$

$$Nd_2Zr_2O_7 + 0.44TiO_2 \longrightarrow 1.13Nd_{1.78}Ti_{0.39}Zr_{1.78}O_7 \quad (15)$$

The displacement of ZrO_2 is first detected between 0.56 and 0.70 mol of TiO_2 reacted. The slope of the line representing preparations displacing ZrO_2 (Line B) is not as steep as the one where no ZrO_2 was displaced. In the solid solutions formed from these preparations, only the concentrations of titanium and zirconium are changing; this is illustrated in Equations (16)-(18), assuming that addition of TiO_2 beyond 0.62 mol results in displacement of ZrO_2.

$$Nd_2Zr_2O_7 + 0.62TiO_2 \longrightarrow 1.18Nd_{1.70}Ti_{0.53}Zr_{1.70}O_7 \quad (16)$$

$$Nd_2Zr_2O_7 + 0.70TiO_2 \longrightarrow 1.18Nd_{1.70}Ti_{0.59}Zr_{1.64}O_7 + 0.07ZrO_2 \quad (17)$$

$$Nd_2Zr_2O_7 + 1.27TiO_2 \longrightarrow 1.18Nd_{1.70}Ti_{1.08}Zr_{1.15}O_7 + 0.64ZrO_2 \quad (18)$$

A third line (Line C) can be drawn for the region between 1.5 and 2 mol of TiO_2 reacted. Here, the volume of the solid solution is not changing greatly with increasing amount of TiO_2 reacted, because the solid solution becomes saturated with TiO_2, and $Zr_{1-x}Ti_xO_2$, as detected by XRD, is displaced instead of pure ZrO_2.

Reaction of $Nd_2Ti_2O_7$ with varying amounts of ZrO_2 did not result in the formation of a single-phase compound. Instead, the XRD data from the preparations indicated that a cubic pyrochlore-type and $Nd_2Ti_2O_7$ were present.

Based on the findings from the study of the systems $Nd_2Ti_2O_7$-$Nd_2Zr_2O_7$, $Nd_2Zr_2O_7$-TiO_2, and $Nd_2Ti_2O_7$-ZrO_2 and other compositions not included in these systems, a region of single-phase pyrochlore-type solid solutions was identified in the ternary system $NdO_{1.5}$-TiO_2-ZrO_2. This region of solid solution formation and other compositions studied to define the region are shown in the ternary phase diagram in Figure 16.

F. Attempts to Substitute Zirconium for Titanium in the Perovskite-Type Phases $SrLn_2Ti_4O_{12}$ and $Sr_2Ce_2Ti_5O_{16}$

Perovskite-type solid solution formation has been reported for the system $Na_2La_2Ti_{4-y}Zr_yO_{12}$ at any composition [21]. Thus, attempts were made to prepare the zirconium analog of $SrLn_2Ti_4O_{12}$ in which Ln=Nd, Gd, or Lu (Equation (19)). A single phase product did not form for any Ln.

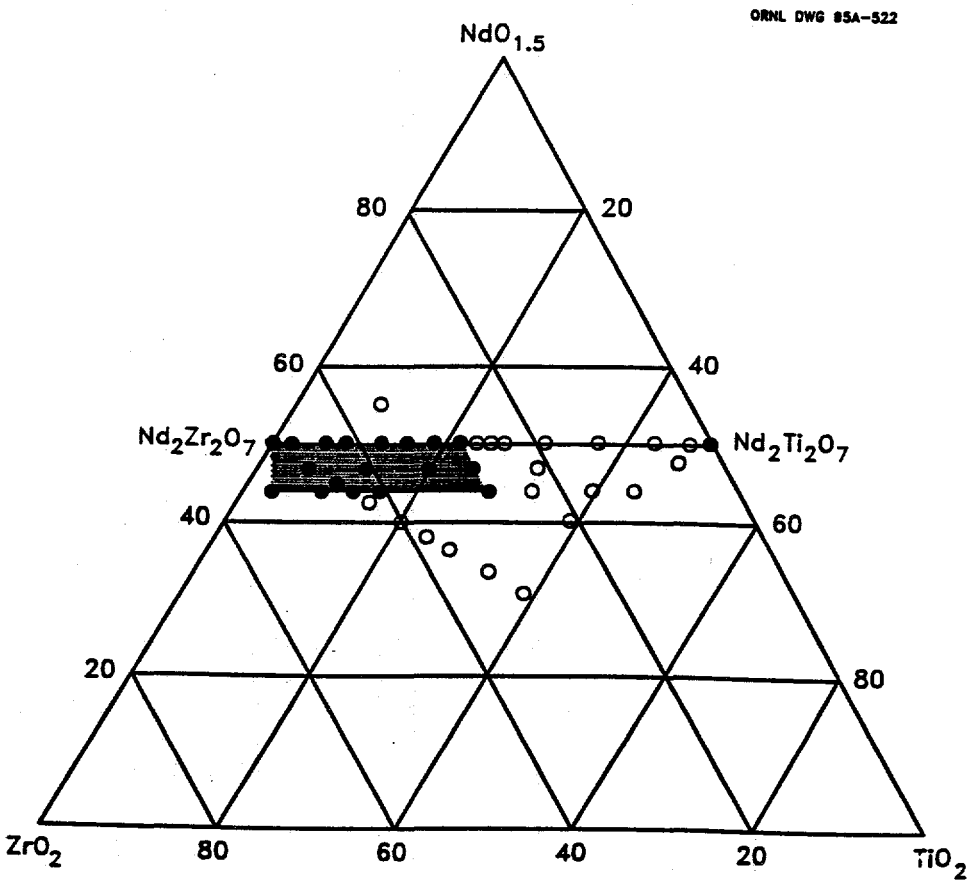

Figure 16. Phase Diagram for $NdO_{1.5}$-TiO_2-ZrO_2 between 1400 and 1500°C.
●: Single Phase; O: More than One Phase; Shaded Area Indicates a Region of Solid Solution Homogeneity.

Instead the products $SrZrO_3$, ZrO_2, and $Ln_2Zr_2O_7$ were detected using XRD. Subsequently, mixtures in which only part of the titanium was replaced by zirconium, e.g., $SrNd_2Ti_{4-y}Zr_yO_{12}$, where y=0.2, 0.4, 0.8, and 1.2 (Equations (20)-(23)), were calcined but still did not result in the formation of a single phase compound. For all of the compositions, a perovskite-type compound and a pyrochlore-type compound were identified in the XRD data. The preparation where y=0.8 also had ZrO_2 present, while the preparation where y=1.2 showed ZrO_2 and $Nd_2Ti_2O_7$ as well.

$$SrO + Ln_2O_3 + 4ZrO_2 \rightarrow SrZrO_3 + ZrO_2 + Ln_2Zr_2O_7 \qquad (19)$$

$$SrO + Nd_2O_3 + 3.8TiO_2 + 0.2ZrO_2 \rightarrow \begin{matrix}\text{a perovskite-type phase=Pe} \\ + \\ \text{a pyrochlore-type phase=Py}\end{matrix} \qquad (20)$$

$$SrO + Nd_2O_3 + 3.6TiO_2 + 0.4ZrO_2 \rightarrow \begin{matrix}Pe' \\ + \\ Py'\end{matrix} \qquad (21)$$

$$SrO + Nd_2O_3 + 3.2TiO_2 + 0.8ZrO_2 \rightarrow \begin{matrix}Pe'' \\ + \\ Py'' + xZrO_2\end{matrix} \qquad (22)$$

$$SrO + Nd_2O_3 + 2.8TiO_2 + 1.2ZrO_2 \rightarrow \begin{matrix}Pe''' \\ + \\ Py''' \\ + \\ x'ZrO_2 + yNd_2Ti_2O_7\end{matrix} \qquad (23)$$

The perovskite-type compound seems to be similar to members of the series $Sr_{4-x}Nd_{2x/3}Ti_4O_{12}$, while the pyrochlore-type compound is similar to members of the system $Nd_2Zr_2O_7$-TiO_2 discussed above. No superstructure lines are seen in the XRD data for the perovskite-type phase, suggesting that, if the compounds are related to the series $Sr_{4-x}Nd_{2x/3}Ti_4O_{12}$, x is most likely smaller than 2.84. The compositions of the pyrochlore-type compounds are most likely similar to compositions of pyrochlore-type compounds such as those given in Equations (14-18) based on the similar volumes measured for both series of compounds.

Attempts to correlate, using mass balance calculations, approximate compositions of the perovskite-type compounds assuming no zirconium substitution (obtained from measured volumes and Figure 8, Chapter IV) and the pyrochlore-type compounds (obtained from measured volumes and compositions similar to those given in Equations (14-18)) to the original composition of the mixture were not successful (see Appendix C for example calculation). This suggests that the measured volumes of the compounds do not correspond to the compositions previously known, possibly indicating the presence of a small amount of zirconium in the perovskite-type compound and/or a different composition of the pyrochlore-type compound ($Nd_aTi_bZr_cO_7$) than seen previously. Ultimately, there are too many unknown variables, such as quotients indicating relative amounts and subscripts

indicating compositions, to identify precisely the compositions of both the perovskite- and pyrochlore-type phases.

Some single-phase solid solution formation had been expected in the above-mentioned system based on the behavior of the series $Na_2La_2Ti_{4-y}Zr_yO_{12}$ where it was reported that single-phase solid solution formation occurred at any composition [21]. Analysis and interpretation of the data reported in the literature for several compositions in the $Na_2La_2Ti_{4-y}Zr_yO_{12}$ system indicated that at y=0.4 a single-phase, perovskite-type solid solution had been formed. However, as the amount of zirconium substituted for titanium increased, the total number of diffraction lines in the data increased, and data similar to that expected for a pyrochlore-type compound, such as $La_2Zr_2O_7$, appeared. This suggests that single-phase, perovskite-type solid solution formation only occurs at low concentrations of zirconium in the series $Na_2La_2Ti_{4-y}Zr_yO_{12}$ in contrast to what has been previously reported.

Attempts to replace titanium by zirconium in $Sr_2Ce_2Ti_5O_{16}$ also were unsuccessful. Present in the XRD data of a composition equivalent to $Sr_2Ce_2Zr_5O_{16}$ were $SrZrO_3$, $Ce_{0.6}Zr_{0.4}O_2$, and $Zr_{0.84}Ce_{0.16}O_2$ (Equation (24)).

$$2SrO + 2CeO_2 + 5ZrO_2 \longrightarrow \begin{matrix} 2SrZrO_3 \\ + \\ xCe_{0.6}Zr_{0.4}O_2 + yZr_{0.84}Ce_{0.16}O_2 \end{matrix} \quad (24)$$

In the series $Sr_2Ce_2Ti_{5-y}Zr_yO_{16}$, where y=0.25, 0.5, 1.0, and 1.5, no single phases were seen in the XRD data. Instead perovskite-type phases similar to $Sr_{6-12x}Ce_{6x}Ti_5O_{16}$ were seen along with $Ce_{1-x}Zr_xO_2$ compounds. Based on the same observations described above, it is possible that some of the zirconium did indeed replace titanium. It is also likely that there is also some substitution of titanium for zirconium in the $Ce_{1-x}Zr_xO_2$ compounds. Similar to the $SrNd_2Ti_{4-y}Zr_yO_{12}$ system, there are just too many unknown variables in this system to determine by calculation the exact compositions of the products.

CHAPTER VI

SOLUBILITY STUDIES OF REPRESENTATIVE COMPOUNDS AND SOLID SOLUTIONS

A. Introduction

Establishing the existence of compounds that can incorporate elements of interest is only the first step in suggesting the use of such compounds as waste host matrices for radioactive elements. The durability of a compound with respect to leaching is an equally important consideration.

The Materials Characterization Center (MCC) has developed a number of procedures specifically designed to determine a compound's solubility or leaching rate under different experimental conditions [36]. Following these procedures makes it possible to compare directly the results obtained by several research groups. Modified MCC-3 procedures [36] were used in this work to study the solubility of selected compounds and solid solutions.

Five lanthanide-containing compounds and solid solutions and two actinide-containing solid solutions were selected as representatives of the systems studied to be the subjects of these solubility tests. The lanthanide-containing compounds and solid solutions studied were $Ce_2Ti_2O_7$, $Er_{1.78}Ce_{0.22}Ti_2O_7$, $Er_{1.78}Ce_{0.22}Ti_{0.5}Zr_{1.5}O_7$, $SrCe_2Ti_4O_{12}$, and $Sr_2Ce_2Ti_5O_{16}$. The actinide-containing solid solutions were

$Er_{1.78}Pu_{0.22}Ti_2O_7$ and $SrPu_2Ti_4O_{12}$.

The solubilities of the lanthanide-containing compounds and solid solutions in four leachants were investigated. The leachants were WIPP "A" brine [38], a synthetic substitute for that found in nature at the WIPP site in New Mexico, 0.1 M NaCl solution, used as a constant ionic strength solution, 0.1 M HCl solution, and 6.0 M HCl solution, used to determine the "maximum solubility" of and structural damage to the compounds and solid solutions. The solubilities of the plutonium-containing solid solutions were studied only in WIPP "A" brine and 6.0 M HCl solution. The solubility experiments were performed at two temperatures, room temperature and 50°C for the lanthanide-containing solids, and at room temperature only for the plutonium-containing solids.

The compounds and solid solutions were in contact with the leachants for eight weeks, a reasonable contact time, based on several other studies using MCC procedures [25,34,37], for preliminary solubility results. At the end of this eight-week period, aliquots of each leachate were analyzed; leachates from lanthanide-containing solids by ICP atomic emission spectrometry for cerium, erbium, strontium, titanium, and zirconium and leachates from plutonium-containing solids by gross alpha counting and alpha pulse height analysis for plutonium only. The detection limits established for each element in the different leachants are

given in Table IX.

No dramatic changes in pH were found for the leachates from the lanthanide-containing solids compared to the solutions before contact with the compounds and solid solutions except in the case of the strontium-containing 0.1 M NaCl leachates. The pH of these leachates was higher than that of the 0.1 M NaCl solution measured before contact with the solids.

Samples of the cerium-containing solids remaining after the solubility tests at 50°C were analyzed by XRD to determine if the compounds had sustained any structural damage detectable by XRD and, if possible, the identity of any new phases resulting from the degradation. When comparing concentrations, given in ppm (mg/L solution), of elements leached with the results seen from these XRD data, it is important to keep in perspective the relative magnitudes of the concentration leached and the mass percent of the total compound or solid solution dissolved. For example, concentrations totalling 300 ppm for a given compound or solid solution resulted from the dissolution of about 0.3% of the compound (based on the original 20 mL of solution and 2.0 grams of solid). Concentrations totalling 1500 ppm resulted from the dissolution of 1.5% of the solid, and concentrations totalling 10000 ppm resulted from the dissolution of 10% of the solid.

Table IX

Detection Limits Established for Each Element in the Different Leachants*

	Strontium (ppm)	Erbium (ppm)	Cerium (ppm)	Titanium (ppm)	Zirconium (ppm)
WIPP "A" Brine	1	0.1	10	0.1	0.04
0.1 M NaCl	1	4	2	3	1
0.1 M HCl	0.001	0.01	0.2	0.002	0.004
6.0 M HCl	0.06	0.03	0.6	0.01	0.06

*These limits of detection (except for cerium in the brine solution) were taken as three times the standard deviation of the concentration of each element measured in the blank leachants. The limit of detection for cerium in the blank brine solution was determined based on the instrumental reading, which greatly exceeded its standard deviation.

B. Solubility Test Results for $Ce_2Ti_2O_7$

The compound $Ce_2Ti_2O_7$ was selected for study to give an idea of the aqueous solubility of the monoclinic dititanates because no such reports have been found in the literature. The concentrations of elements present in the different leachates held at both test temperatures, as determined by ICP and reported as ppm (or mg/L solution), are given in Table X. The amounts of cerium and titanium leached by both WIPP brine and 0.1 M NaCl solutions were below the detection limits (BDL) found for these solutions in the ICP spectrometer. Cerium and titanium were dissolved by 0.1 M HCl solution at room temperature, but only cerium was detected in the leachate held at 50°C. An accurate concentration of titanium could not be obtained because upon dilution of the leachate for analysis, a white solid believed to contain titanium precipitated. The 6.0 M HCl solution proved to be quite corrosive to $Ce_2Ti_2O_7$, leaching significant amounts of cerium at both temperatures. The amounts were so high that accurate concentrations could not be obtained using the experimental calibration curves established for this leachant. No accurate concentration of titanium could be obtained because of the precipitation problem upon dilution discussed above.

Analysis of the XRD results from solids remaining after contact with the leachants at 50°C are given in Table XI. The results from the sample in the brine solution indicate

Table X

Concentrations of Elements Leached from $Ce_2Ti_2O_7$ by the Different Leachants at the Two Test Temperatures

		Cerium (ppm)	Titanium (ppm)
WIPP Brine	RT	BDL	BDL
	50°C	BDL	BDL
0.1 M NaCl	RT	BDL	BDL
	50°C	BDL	BDL
0.1 M HCl	RT	301±32	(1)
	50°C	305±133	BDL
6.0 M HCl	RT	> 13468 (2)	(1)
	50°C	> 14476 (2)	(1)

BDL = Below Detection Limits

(1) An accurate concentration of titanium could not be obtained because a solid believed to contain titanium precipitated upon dilution.

(2) An accurate concentration of cerium could not be obtained because the amount in solution was greater than that which could be fitted to the established calibration curve.

Table XI

XRD Results Obtained from the Remaining Solid Present after the Leaching of $Ce_2Ti_2O_7$ by the Different Leachants at 50°C

	XRD Results
WIPP Brine	major phase:$Ce_2Ti_2O_7$; significant amount of pyrochlore-type phase
0.1 M NaCl	no change
0.1 M HCl	no change
6.0 M HCl	$Ce_2Ti_2O_7$, TiO_2, and CeO_2

that the major phase of the solid present after contact is still $Ce_2Ti_2O_7$; however, significant amounts of a pyrochlore-type phase are also present. This can be explained by considering that small amounts of Ce(III) could have been oxidized to Ce(IV) allowing the radius ratio of the Ce(III) and Ce(IV) to Ti(IV) ions present to fall within the range necessary for pyrochlore formation. Solids that had been in contact with 0.1 M NaCl and 0.1 M HCl solutions showed no changes by XRD. The sample in contact with 6.0 M HCl solution had significant amounts of Ce(III) oxidized to insoluble CeO_2, as seen in the XRD data. Also present were significant amounts of TiO_2 and the initial compound $Ce_2Ti_2O_7$.

C. Solubility Test Results for $Er_{1.78}Ce_{0.22}Ti_2O_7$

The solid solution $Er_{1.78}Ce_{0.22}Ti_2O_7$ was selected for study to compare the aqueous solubility found for $Ce_2Ti_2O_7$ to that of a solid solution of $Ce_2Ti_2O_7$ in a pyrochlore-type heavy lanthanide dititanate. The concentrations of elements present in the leachates, as determined by ICP, are given in Table XII. As seen for $Ce_2Ti_2O_7$, the concentrations of cerium and titanium leached in the brine and 0.1 M NaCl solutions are below the detection limits of the ICP spectrometer. Significant amounts of erbium were leached by the 0.1 M HCl solution. The 6.0 M HCl solution leached erbium, cerium, and titanium. Upon dilution of this

Table XII

Concentrations of Elements Leached from $Er_{1.78}Ce_{0.22}Ti_2O_7$ by the Different Leachants at the Two Test Temperatures

		Erbium (ppm)	Cerium (ppm)	Titanium (ppm)
WIPP Brine	RT	16±1	BDL	BDL
	50°C	11±1	BDL	BDL
0.1 M NaCl	RT	BDL	BDL	BDL
	50°C	BDL	BDL	BDL
0.1 M HCl	RT	1308±2	96±1	11±1
	50°C	1367±10	136±1	3±1
6.0 M HCl	RT	1650±68	218±3	(1)
	50°C	1252±392	218±1	(1)

BDL = Below Detection Limits

(1) An accurate concentration of titanium could not be obtained because a solid believed to contain titanium precipitated upon dilution.

leachate, precipitation occurred, and therefore an accurate value for titanium leached at either temperature cannot be given.

The XRD results of the solids remaining after the 50°C test, listed in Table XIII, indicate that no major structural damage was done to the samples in any of the leachants, even 6.0 M HCl solution. There was virtually no change detected in the XRD results of the solids previously in contact with the leachants compared to the results of $Er_{1.78}Ce_{0.22}Ti_2O_7$ before leaching. The XRD data from the solid remaining after contact with 0.1 M NaCl solution showed one extra, very low intensity line not attributable to $Er_{1.78}Ce_{0.22}Ti_2O_7$. This single line corresponds to the most intense peak in the XRD pattern of $Ce_2Ti_3O_{9-3m}$, but an unambiguous identification cannot be made based on one line. Likewise, the XRD data from the solid remaining after contact with 0.1 M HCl solution showed one additional, very low intensity line, possibly from TiO_2, but there were insufficient data to identify unambiguously an extra phase.

D. Solubility Test Results for $Er_{1.78}Ce_{0.22}Ti_{0.5}Zr_{1.5}O_7$

The solid solution $Er_{1.78}Ce_{0.22}Ti_{0.5}Zr_{1.5}O_7$ was selected to determine the influence of zirconium on the aqueous solubility of a solid solution compared to that of $Er_{1.78}Ce_{0.22}Ti_2O_7$. The concentrations of erbium, cerium, titanium, and zirconium, as determined by ICP, are listed in

Table XIII

XRD Results Obtained from the Remaining Solid Present after the Leaching of $Er_{1.78}Ce_{0.22}Ti_2O_7$ by the Different Leachants at 50°C

	XRD Results
WIPP Brine	no change
0.1 M NaCl	major phase: $Er_{1.78}Ce_{0.22}Ti_2O_7$; very small amount of $Ce_2Ti_3O_{9-3m}$ questionable
0.1 M HCl	major phase: $Er_{1.78}Ce_{0.22}Ti_2O_7$; very small amount of TiO_2 questionable
6.0 M HCl	no change

Table XIV. The elements leached by the brine and 0.1 M NaCl solutions were slightly above or below the detection limits and were comparable to the concentrations of erbium, cerium, and titanium leached from $Er_{1.78}Ce_{0.22}Ti_2O_7$. The amounts of erbium, cerium, and titanium leached by 0.1 M and 6.0 M HCl solutions were also comparable to those leached from $Er_{1.78}Ce_{0.22}Ti_2O_7$. Therefore, zirconium does not seem to have much of an effect on the overall solubility of such solid solutions.

The XRD results obtained from the solids remaining after the 50°C test, listed in Table XV, do not differ much from the results of $Er_{1.78}Ce_{0.22}Ti_{0.5}Zr_{1.5}O_7$ before leaching. Only the data from the solid which had been in contact with the brine solution show any change. A small amount of a phase identified as $Ce_2Ti_3O_{9-3m}$ was detected in addition to the main phase of $Er_{1.78}Ce_{0.22}Ti_{0.5}Zr_{1.5}O_7$. This is reasonable because some Ti(III) is likely present since the solid solution was calcined in Ar/4% H_2.

E. Solubility Test Results for $SrCe_2Ti_4O_{12}$

The compound $SrCe_2Ti_4O_{12}$, a member of the series $Sr_{4-x}Ce_{2x/3}Ti_4O_{12}$, where x=3.0 and cerium is in the III oxidation state, was selected to determine its potential as a host matrix for ^{90}Sr. The concentrations of the elements present in the leachates, determined by ICP, are given in Table XVI. In the case of the brine and 0.1 M NaCl

Table XIV

Concentrations of Elements Leached from $Er_{1.78}Ce_{0.22}Ti_{0.5}Zr_{1.5}O_7$ by the Different Leachants at the Two Test Temperatures

		Erbium (ppm)	Cerium (ppm)	Titanium (ppm)	Zirconium (ppm)
WIPP Brine	RT	20±1	BDL	BDL	BDL
	50°C	16±1	BDL	BDL	BDL
0.1 M NaCl	RT	BDL	BDL	BDL	BDL
	50°C	BDL	BDL	BDL	BDL
0.1 M HCl	RT	1196±16	53±1	28±1	20±1
	50°C	1198±9	46±7	16±1	BDL
6.0 M HCl	RT	1705±6	198±1	125±2	129±1
	50°C	1802±113	272±4	134±9	327±5

BDL = Below Detection Limit

Table XV

XRD Results Obtained from the Remaining Solid Present after the Leaching of $Er_{1.78}Ce_{0.22}Ti_{0.5}Zr_{1.5}O_7$ by the Different Leachants at 50°C

	XRD Results
WIPP Brine	major phase: $Er_{1.78}Ce_{0.22}Ti_{0.5}Zr_{1.5}O_7$; small amount of $Ce_2Ti_3O_{9-3m}$
0.1 M NaCl	no change
0.1 M HCl	no change
6.0 M HCl	no change

Table XVI

Concentrations of Elements Leached from $SrCe_2Ti_4O_{12}$ by the Different Leachants at the Two Test Temperatures

		Strontium (ppm)	Cerium (ppm)	Titanium (ppm)
WIPP Brine	RT	33±1	BDL	BDL
	50°C	26±1	BDL	BDL
0.1 M NaCl	RT	> 5586 (3)	BDL	BDL
	50°C	> 4594 (3)	BDL	BDL
0.1 M HCl	RT	139±1	294±1	(1)
	50°C	81±1	153±2	29±1
6.0 M HCl	RT	785±37	2015±246	(1)
	50°C	9708±216	> 11248 (2)	522±7

BDL = Below Detection Limits

(1) An accurate concentration of titanium could not be obtained because a solid believed to contain titanium precipitated upon dilution.

(2) An accurate concentration of cerium could not be obtained because the amount in solution was greater than that which could be fitted to the established calibration curve.

(3) An accurate concentration of strontium could not be obtained because the amount in solution was greater than that which could be fitted to the established calibration curve.

solutions, the concentrations of cerium and titanium detected in the leachates are below the detection limits of the ICP spectrometer; however, the amounts of strontium leached by these two solutions differ significantly. An accurate concentration of strontium leached by 0.1 M NaCl could not be obtained because the amount in solution was greater than that which could be fitted to the calibration curve established for strontium in 0.1 M NaCl. Strontium, cerium, and titanium are leached by 0.1 M HCl solution, but the concentration of titanium could not be accurately obtained in the leachate held at room temperature because of the precipitation problem mentioned before. Significant amounts of strontium, cerium, and titanium are leached by 6.0 M HCl solution. The concentration of cerium in the leachate held at 50°C could not be accurately determined as the value was too high to fit on the calibration curve. The concentration of titanium is not accurately known in the leachate held at room temperature because of the precipitation problem upon dilution previously discussed.

The results of the XRD analysis of the solids remaining after the 50°C test are given in Table XVII. The results from the sample which had been in contact with the brine solution indicate that the major phase present is $SrCe_2Ti_4O_{12}$. There are two additional phases present, a $Ce_2Ti_2O_7$-type phase, having a smaller volume than that of pure $Ce_2Ti_2O_7$, and another phase, possibly a titanium

Table XVII

XRD Results Obtained from the Remaining Solid Present after the Leaching of $SrCe_2Ti_4O_{12}$ by the Different Leachants at 50°C

	XRD Results
WIPP Brine	major phase: $SrCe_2Ti_4O_{12}$; small amounts of $Ce_2Ti_2O_7$-type phase and titanium suboxide phase questionable
0.1 M NaCl	major phase: $SrCe_2Ti_4O_{12}$; very small amount of $Ce_2Ti_2O_7$ questionable
0.1 M HCl	no change
6.0 M HCl	major phase: TiO_2; significant amount of $SrCeO_3$ questionable

suboxide, both resulting from the small amount of strontium soluble in the brine solution. The reduced titanium species is likely because the compound was originally calcined in Ar/4% H_2, possibly allowing reduction of some Ti(IV) to Ti(III). The sample in contact with 0.1 M NaCl solution remained virtually unchanged; additionally the main diffraction line from $Ce_2Ti_2O_7$ was also seen in the XRD data with a very low intensity. With the significant amount of strontium dissolved, the presence of $Ce_2Ti_2O_7$ is quite likely. No change was seen for the sample which had been in contact with 0.1 M HCl solution, but the sample leached in 6.0 M HCl solution was totally destroyed leaving TiO_2 as the main phase and a significant amount of another phase present, possibly $SrCeO_3$. This would have required that all the remaining Ce(III) be oxidized to Ce(IV), which is possible in the high acidity medium.

F. Solubility Test Results for $Sr_2Ce_2Ti_5O_{16}$

The compound $Sr_2Ce_2Ti_5O_{16}$, a member of the solid solution series $Sr_{6-12x}Ce_{6x}Ti_5O_{16}$ where x=0.33 and cerium is in the IV oxidation state, was selected to compare the stability of this strontium-containing compound to that of $SrCe_2Ti_4O_{12}$ with Ce(III) discussed above. The concentrations of elements determined present in the leachates by ICP are given in Table XVIII. As seen for $SrCe_2Ti_4O_{12}$, the concentrations of cerium and titanium in the leachates are

Table XVIII

Concentrations of Elements Leached from $Sr_2Ce_2Ti_5O_{16}$ by the Different Leachants at the Two Test Temperatures

		Strontium (ppm)	Cerium (ppm)	Titanium (ppm)
WIPP Brine	RT	55±1	BDL	BDL
	50°C	42±1	BDL	BDL
0.1 M NaCl	RT	> 8136 (3)	BDL	BDL
	50°C	> 7048 (3)	BDL	BDL
0.1 M HCl	RT	220±1	159±1	(1)
	50°C	188±1	106±1	36±1
6.0 M HCl	RT	1279±148	2394±114	(1)
	50°C	> 12940 (3)	> 8996 (2)	(1)

BDL = Below Detection Limits

(1) An accurate concentration of titanium could not be obtained because a solid believed to contain titanium precipitated upon dilution.

(2) An accurate concentration of cerium could not be obtained because the amount in solution was greater than that which could be fitted to the established calibration curve.

(3) An accurate concentration of strontium could not be obtained because the amount in solution was greater than that which could be fitted to the established calibration curves.

below the detection limits. There is a significant difference between the amounts of strontium leached by the brine and 0.1 M NaCl solutions as there was for $SrCe_2Ti_4O_{12}$. No accurate concentration of strontium could be obtained in the leachate held at either temperature because the amounts in solution were greater than that which could be fitted to the established calibration curve. Strontium, cerium, and titanium were detected in the leachates of 0.1 M HCl solution, but the concentration of titanium can not be accurately determined for the room temperature leachate because of the precipitation problem upon dilution. The 6.0 M HCl solution, especially at 50°C, was quite corrosive to $Sr_2Ce_2Ti_5O_{16}$. No accurate concentration of strontium or cerium could be obtained in the leachate held at 50°C because the amounts in solution were greater than that which could be fitted to the established calibration curves. Because of the precipitation problem discussed previously, no accurate concentration of titanium could be obtained for the sample held at either temperature.

Analysis of the XRD data from the solids remaining from the test at 50°C gave the results listed in Table XIX. No major structural damage had occurred to the compound in the WIPP "A" brine, 0.1 M NaCl, or 0.1 M HCl solutions. The XRD data from the solid remaining after contact with 6.0 M HCl solution indicated that although the main phase present was that of $Sr_2Ce_2Ti_5O_{16}$, a significant amount of TiO_2 was also

Table XIX

XRD Results Obtained from the Remaining Solid Present after the Leaching of $Sr_2Ce_2Ti_5O_{16}$ by the Different Leachants at 50°C

	XRD Results
WIPP Brine	no change
0.1 M NaCl	no change
0.1 M HCl	no change
6.0 M HCl	major phase: $Sr_2Ce_2Ti_5O_{16}$; significant amount of TiO_2 also present

present.

G. Solubility Test Results for $Er_{1.78}Pu_{0.22}Ti_2O_7$

The solubility of the plutonium from the solid solution $Er_{1.78}Pu_{0.22}Ti_2O_7$ was investigated in WIPP "A" brine and 6.0 M HCl solutions at room temperature. The results from gross alpha counting and alpha pulse height analysis are given in Table XX. Information from an alpha pulse height analysis indicates the alpha emitting radioactive isotopes present in a sample based on the characteristic alpha particle energies detected. The pulse height analysis of the 6.0 M HCl leachate indicated that ^{241}Am was present as an impurity. The concentration of ^{241}Am determined was not included in the leaching results, as it is not known when the sample was contaminated with Am.

The 6.0 M HCl solution dissolved more plutonium than did WIPP brine. The amount of plutonium leached by WIPP brine is most likely comparable to the amount of cerium leached by the WIPP brine from the analog solid solution, $Er_{1.78}Ce_{0.22}Ti_2O_7$. The concentration of cerium determined by ICP was below the limit of detection for cerium in the WIPP brine (10 ppm). The amount of plutonium dissolved by 6.0 M HCl solution was higher than the amount of cerium leached (218 ppm).

Table XX

Concentration of Plutonium Leached from $Er_{1.78}Pu_{0.22}Ti_2O_7$ by the Two Different Leachants at Room Temperature

	Plutonium (ppm)
WIPP "A" brine	0.2±0.1
6.0 M HCl	890±87

H. Solubility Test Results for $SrPu_2Ti_4O_{12}$

The solubility of the plutonium from the solid solution $SrPu_2Ti_4O_{12}$ was investigated in WIPP "A" brine and 6.0 M HCl solutions at room temperature. The results from gross alpha counting and alpha pulse height analysis are given in Table XXI. The pulse height analysis of the 6.0 M HCl leachate indicated that ^{241}Am and ^{239}Pu were present as impurities. The concentrations of these impurities were not included in the leaching results because it is not known when the sample was contaminated.

The 6.0 M HCl solution dissolved a significant amount of plutonium compared to WIPP brine. The amounts of cerium and plutonium leached by WIPP "A" brine from $SrM_2Ti_4O_{12}$ (M=Ce or Pu) may very well be comparable because the concentration of cerium leached was below the detection limit (10 ppm). The system was considered saturated with cerium leached by 6.0 M HCl solution indicating that a very large amount was present. This is also true for the plutonium leached by 6.0 M HCl solution.

I. Conclusions Regarding the Solubility Tests

Although there are limitations and difficulties in using ICP to analyze such complex matrices as the leachants used in this work, preliminary solubility data have been gathered for several systems of cerium-containing compounds and solid solutions that could prove useful in immobilizing

Table XXI

Concentration of Plutonium Leached from $SrPu_2Ti_4O_{12}$ by the Two Different Leachants at Room Temperature

	Plutonium (ppm)
WIPP "A" brine	0.2±0.1
6.0 M HCl	58970±1795

radioactive elements. Temperature variation between room temperature and 50°C seemed to have no significant effect on the leachability of the elements in any of the leachants except 6.0 M HCl. The WIPP brine was the most realistic leachant used, and thus conclusions regarding the potential usefulness of these compounds and solid solutions as host matrices should be drawn from the leaching data using the brine solution. Overall, all of the compounds and solid solutions fared well in WIPP brine with concentrations of cerium, as a surrogate for plutonium, below the ICP detection limit established for WIPP brine. Even the concentrations of stable strontium, used as a surrogate for ^{90}Sr, were quite low. The solubility tests on the plutonium-containing solid solutions showed concentrations of less than 1 ppm leached by the brine and were comparable to the concentrations found for cerium in the analogous solid solutions.

CHAPTER VII

SUMMARY AND CONCLUSIONS

The purpose of this work was to investigate novel compound and solid solution formation in lanthanide- and actinide-containing titanate and zircono-titanate systems using X-ray diffraction. Representative compounds from the systems studied were subjected to solubility tests to evaluate their potential as matrices for immobilizing nuclear waste.

First, pure titanate compounds and solid solutions were investigated. The actinide dititanates $Pu_2Ti_2O_7$ and $Am_2Ti_2O_7$ were prepared and characterized by XRD. They were found to exhibit a monoclinic structure like their light lanthanide analogs, $Ln_2Ti_2O_7$, and to be soluble in the cubic pyrochlore-type, heavy lanthanide dititanates, $Ln'_2Ti_2O_7$. The limits of solid solubility of $Pu_2Ti_2O_7$ in $Ln'_2Ti_2O_7$ hosts where Ln'=Gd, Er, or Lu were estimated as 16±4, 22±3, 33±3 mol percent, respectively. These values agree well with those found for the solubility of $Ce_2Ti_2O_7$ in these same cubic $Ln'_2Ti_2O_7$ hosts (19, 22, and 27 mol percent, respectively) [7]. This agreement was expected given the similarities in radii of Pu(III) and Ce(III). The limit of solid solubility of $Am_2Ti_2O_7$ in $Er_2Ti_2O_7$ was estimated to be 59±9 mol percent. This value agrees well, as expected based on ionic radii,

with that found for $Nd_2Ti_2O_7$ in $Er_2Ti_2O_7$ (60.7 mol percent) [6].

The solubility limits of TiO_{2-m} in $Ln_2O_3 \cdot (nTiO_{2-m})$ were determined. It was found that compounds of the type $Ln_2O_3 \cdot (3TiO_{2-m})$ with Ln=La or Nd can incorporate an additional 0.5 mol of TiO_{2-m} isomorphously to form $Ln_2O_3 \cdot (3.5TiO_{2-m})$. With Ln=Pr, an additional 1.0 mol of TiO_2 is accommodated to form $Ln_2O_3 \cdot (4TiO_{2-m})$. The compound $Pu_2O_3 \cdot (3TiO_{2-m})$ was prepared and characterized using XRD. Oxidation reactions of several such lanthanide-containing compounds indicated that $m \approx 0.16$. The value of m for the plutonium-containing compound was found to be approximately 0.07.

A series of titanate solid solutions that would incorporate strontium and a light lanthanide had been reported, but there was disagreement in the literature about the range of solid solubility and the crystal structure of the solid solutions [14-16,46,47]. The system $SrO-LnO_{1.5}-TiO_2$ was reinvestigated emphasizing Ln=Ce, for which no results had been reported, and Nd. A series of solid solutions, which have the composition $Sr_{4-x}Ln_{2x/3}Ti_4O_{12}$, was found to exist along the tie line between $SrTiO_3$ and $Ln_2Ti_3O_{9-3m}$ for Ln=La, Ce, Pr, or Nd. These solid solutions below 45±5 mol percent $Ln_2Ti_3O_{9-3m}$ were interpreted to have cubic (slightly distorted to tetragonal) perovskite-type structures. The structure of the solid solutions above 45±5 mol percent $Ln_2Ti_3O_{9-3m}$, including $SrLn_2Ti_4O_{12}$, selected as the

representative compound of the series, was interpreted to have a tetragonally distorted perovskite-type structure.

Reactions between $SrLn_2Ti_4O_{12}$ and 1 mol of SrO resulted in $Sr_{4-x}Ln_{2x/3}Ti_4O_{12}$ ($x \leq 0.5$) and $Ln_2Ti_2O_7$ for Ln=La, Ce, Pr, or Nd. Reactions between $SrNd_2Ti_4O_{12}$ and 3, 5, or 7 mol of SrO produced Nd_2O_3 and strontium titanates.

With the series $Sr_{4-x}Ln_{2x/3}Ti_4O_{12}$ defined, the actinide analogs where x=3.0, $SrPu_2Ti_4O_{12}$ and $SrAm_2Ti_4O_{12}$, were prepared and characterized by XRD as tetragonally distorted perovskite-type phases. The existence of the perovskite-type $Sr_2Ce_2Ti_5O_{16}$, where cerium is in the IV oxidation state, led to attempts to synthesize the An(IV) (An=Np-Am) analogs, $Sr_2An_2Ti_5O_{16}$, and solid solutions of the type $Sr_2Ce_{2-y}An_yTi_5O_{16}$ (An=Np or Pu). These attempts were unsuccessful. Although Ce(IV) and the An(IV) radii are quite similar, it appears that ionic size is not the controlling parameter in the inability to form these An(IV) compounds. While there is no adequate explanation at this time for the difference in behavior between Ce(IV) and An(IV) with regard to the formation of $Sr_2M_2Ti_5O_{16}$ (M=Ce or An), this case suggests that Ce(IV) may not be an adequate surrogate for An(IV), especially Pu(IV).

The ability to synthesize Pu(III) compounds indicated that TiN was a good reductant for Pu(IV) and is compatible with titanate systems. It was found that calcination in Ar between 1200 and 1300°C was sufficient to reduce Am(IV) to

Am(III). Comparison of the solubilities of $Ce_2Ti_2O_7$ and $Pu_2Ti_2O_7$ in $Ln'_2Ti_2O_7$ and that of $Nd_2Ti_2O_7$ and $Am_2Ti_2O_7$ in $Er_2Ti_2O_7$ and the synthesis of several Pu(III) and Am(III) compounds analogous to Ce(III) and Nd(III) compounds, respectively, confirmed the adequacy of using Ce(III) as a surrogate for Pu(III) and Nd(III) as a surrogate for Am(III). No analogous Np(III) compounds could be formed suggesting that Np(III) is not stable in the titanate matrices studied. The formation of solid solutions of the type $Ln'_{2-x}An_xTi_2O_7$ and of $SrAn_2Ti_4O_{12}$ (An=Pu or Am) suggests that these materials may be suitable matrices for the immobilization of both ^{90}Sr and An(III).

Because of the paucity of information available on complex lanthanide-containing titanium and zirconium pyrochlore- and perovskite-type compounds [19-21,59], systems containing both titanium and zirconium were studied for solid solution formation. Complete solubility was found in the pyrochlore-pyrochlore-type systems $Nd_2Zr_2O_7$-$Er_2Ti_2O_7$ and $Nd_2Zr_2O_7$-$Nd_{1.2}Er_{0.8}Ti_2O_7$, which resulted in cubic pyrochlore-type solid solutions. Some solubility of $Nd_2Ti_2O_7$, a monoclinic dititanate, in defect fluorite $Er_2Zr_2O_7$ was observed. The system does not appear to obey Vegard's Law, but only the pyrochlore-type phase is detected in the XRD data. Most likely, the solid solution is saturated with $Nd_2Ti_2O_7$, but small amounts of excess $Nd_2Ti_2O_7$ are not detected because the most intense diffraction line of

$Nd_2Ti_2O_7$ is nearly coincident with the most intense line of the pyrochlore-type phase.

Solid solution formation between $Ce_2Ti_2O_7$ and $Ce_2Zr_2O_7$ was not successful because of the difficulty in maintaining cerium as Ce(III) and titanium as Ti(IV) while allowing sufficient time for equilibrium to be reached. It was determined that there is some solubility of $Nd_2Ti_2O_7$ in $Nd_2Zr_2O_7$. Pyrochlore-type solid solutions, which have the composition $Nd_2Zr_{2-x}Ti_xO_7$, were found to exist up to an x value of approximately 0.86, at which point the solid solution was saturated and monoclinic $Nd_2Ti_2O_7$, in addition to the pyrochlore, was detected in the XRD data.

The systems $Nd_2Zr_2O_7$-TiO_2 and $Nd_2Ti_2O_7$-ZrO_2 were investigated for pyrochlore solid solution formation to help define, along with the previously mentioned $Nd_2Ti_2O_7$-$Nd_2Zr_2O_7$, a region of solid solution formation in the system $NdO_{1.5}$-TiO_2-ZrO_2. Attempts to replace titanium by zirconium in $SrLn_2Ti_4O_{12}$ and $Sr_2Ce_2Ti_5O_{16}$ were not successful.

The aqueous solubilities of several lanthanide- and actinide-containing compounds and solid solutions, representing the systems studied, were determined. The compounds and solid solutions selected for solubility testing were $Ce_2Ti_2O_7$, $Er_{1.78}Ce_{0.22}Ti_2O_7$, $Er_{1.78}Pu_{0.22}Ti_2O_7$, $Er_{1.78}Ce_{0.22}Ti_{0.5}Zr_{1.5}O_7$, $SrCe_2Ti_4O_{12}$, $SrPu_2Ti_4O_{12}$, and $Sr_2Ce_2Ti_5O_{16}$. The solubilities of these compounds and solid solutions at room temperature and/or 50°C in WIPP "A" brine, 0.1 M NaCl,

0.1 M HCl, and 6.0 M HCl solutions were determined. In the leachant imitating a repository setting being considered for the disposal of radioactive waste, i.e., WIPP "A" brine, the concentrations of cerium leached at both temperatures were below the ICP limit of detection (10 ppm) for all of the cerium-containing compounds and solid solutions. The amounts of strontium leached from $SrCe_2Ti_4O_{12}$ and $Sr_2Ce_2Ti_5O_{16}$ by the brine were also quite low. The concentration of plutonium leached from the solid solutions $Er_{1.78}Pu_{0.22}Ti_2O_7$ and $SrPu_2Ti_4O_{12}$ was less than 1 ppm. These preliminary results compare well with those found for cerium in the analog solid solutions and indicate that Ce(III) is a good surrogate for Pu(III) in aqueous solubility studies. Finally, this solubility study suggests that these types of titanate and zircono-titanate compounds and solid solutions might be useful as host matrices for nuclear waste immobilization.

LIST OF REFERENCES

LIST OF REFERENCES

1. N.N. Greenwood and A. Earnshaw, Chemistry of the Elements, Pergamon Press, Oxford (1984).

2. M. Gasperin, Acta Crystallogr., B31 2129-2130 (1975).

3. U. Balachandran and N.G. Eror, J. Mater. Res., 4 1525-1528 (1989).

4. R.A. McCauley and F.A. Hummel, J. Solid State Chem., 33 99-105 (1980).

5. M.A. Subramanian, G. Aravamudan, and G.V. Subba Rao, Prog. Solid St. Chem., 15 55-143 (1983).

6. C.E. Bamberger, H.W. Dunn, G.M. Begun, and S.A.Landry, J. Less-Common Met., 109 209-217 (1985).

7. C.E. Bamberger, T.J. Haverlock, S.S. Shoup, O.C. Kopp, and N.A. Stump, J. Alloys and Compounds, 204 101-107 (1994).

8. A.I. Leonov, M.M. Piryutko, and É.K. Keler, Bull. Acad. Sci. USSR, Div. Chem. Sci., 5 756-760 (1966).

9. G.V. Bazuev, O.V. Makarova and G.P. Shveikin, Russ. J. Inorg. Chem., 23 800-802 (1978).

10. A. Kahn-Harari, Rev. Int. Hautes Temper. et Refract., 8 71-84 (1971).

11. M. Abe and K. Uchino, Mat. Res. Bull., 9 147-156 (1974).

12. C.P. Khattak and F.F.Y. Wang, The Handbook on the Physics and Chemistry of the Rare Earths, eds. K.A. Gschneidner, Jr. and L. Eyring, Elsevier Science Publishers, Amsterdam, 525-607 (1979).

13. V.M. Goldschmidt, Skrifter Norske Videnskaps-Akad. Mat. Naturvid., Kl. No.2 (1926).

14. T.Y. Tien and F.A. Hummel, Trans. Brit. Ceram. Soc., 66 233-245 (1967).

15. J. Bouwma, K.J. de Vries, and A.J. Burggraaf, Phys. Stat. Sol., (a) 35 281-290 (1976).

16. O.V. Sidorova, N.V. Porotnikov, and K.I. Petrov, Russ. J. Inorg. Chem., 27 1107-1108 (1982).

17. C.E. Bamberger, T.J. Haverlock, and O.C. Kopp, J. Amer. Ceram. Soc. 77 1659-1661 (1994).

18. D.F. Shriver, P.W. Atkins, and C.H. Langford, Inorganic Chemistry, W.H. Freeman and Co., New York (1990).

19. P.K. Moon and H.L. Tuller, Solid State Ionics, 28-30 470-474 (1988).

20. C. Heremans, B.J. Wuensch, J.K Stalick, and E. Prince, J. Solid State Chem., 117 108-121 (1995).

21. A.G. Belous, G.N. Novitskaya, L.G. Gavrilova, S.V. Polyanetskaya, and Z. Ya. Makarova, Ukrain. Khimii. Zhurn., 51 13-15 (1985).

22. E.A. Nenasheva, B.A. Rotenberg, E.I. Gindin, and V.G. Prokhvatilov, Inorg. Mater., 16 719-722 (1981).

23. G.T. Seaborg and W.D. Loveland, The Elements Beyond Uranium, John Wiley & Sons, Inc., New York (1990).

24. R.C. Ewing, Radioactive Waste Forms for the Future, eds. W. Lutze & R.C. Ewing, Elsevier Science Publishers, Amsterdam, 589-633 (1988).

25. A.E. Ringwood, S.E. Kesson, N.G. Ware, W. Hibberson, and A. Major, Nature, 278 219-223 (1979).

26. E.R. Vance, MRS Bull., 19 28-32 (1994).

27. K.P. Hart, W.E. Glassley, and P.J. McGlinn, Radiochim. Acta, 58-59 33-35 (1992).

28. E.R. Vance, P.J. Angel, D.J. Cassidy, M.W.A. Stewart, M.G. Blackford, and P.A. McGlinn, J. Am. Ceram. Soc., 77 1576-80 (1994).

29. H.W. Newkirk, C.L. Hoenig, F.J. Ryerson, J.D. Tewhey, G.S. Smith, C.S. Rossington, A.J. Brackmann, and A.E. Ringwood, Ceram. Bull., 61 559-566 (1982).

30. Alternative Waste Form Peer Review Panel, "The Evaluation and Review of Alternative Waste Forms for Immobilization of High Level Radioactive Wastes," Report #3, DOE/TIC-11472 (1981).

31. R.C. Ewing and W. Lutze, MRS Bull., 19 16-18 (1994).

32. G.J. McCarthy, W.B. White, D.K. Smith, and A.C. Lasaga, The Waste Package: Radioactive Waste Disposal, Vol. 1, ed. R. Roy, Pergamon Press, New York, 72-86 (1982).

33. A.E. Ringwood, Safe Disposal of High Level Nuclear Reactor Wastes: A New Strategy, Australia National University Press, Canberra (1978).

34. H.W. Nesbitt, G.M. Bancroft, W.S. Fyfe, S. Karkhanis, P. Melling, and A. Nishijima, Alternate Nuclear Waste Forms and Interactions in Geologic Media, CONF-8005107 25-43 (1981).

35. D. Williams, Rep. IS-1052, Ames Laboratory, Iowa State University, Ames, IA, (1964).

36. Materials Characterization Center, Nuclear Waste Materials Handbook Test Methods (Rev. 6), DOE/TIC 11400 Pacific Northwest Laboratories, Richland, WA (1985).

37. H. Mitamura, S. Matsumoto, M.W.A. Stewart, T. Tsuboi, M. Hashimoto, E.R. Vance, K.P. Hart, Y. Togashi, H. Kanazawa, C.J. Ball and T.J. White, J. Am. Ceram. Soc., 77 2255-64 (1994).

38. R.G. Dosch and A.W. Lynch, Interaction of Radionuclides with Geomedia Associated with the Waste Isolation Pilot Plant Site in New Mexico, SAND78-0297 (1978).

39. "Gross Alpha and Gross Beta Radioactivity in Drinking Water," EPA-600/900.0 (1980).

40. L.H. Brixner, Inorg. Chem., 3 1065-1067 (1964).

41. Powder Diffraction File, Joint Committee for Powder Diffraction Standards, Swarthmore, PA, Card Nos. 18-499 (1968), 23-259 (1973), 23-375 (1973), 28-517 (1978), 33-942 (1983), and 35-267 (1985).

42. F. Queyroux, M. Huber, and R. Collongues, C.R. Acad. Sci., Ser. C, 270 806 (1970).

43. W.E. Klee and G. Weitz, J. Inorg. Nucl. Chem., 31 2367 (1969).

44. O. Knop, F. Brisse, L. Castelliz and Sutarno, Can. J. Chem., 43 2812-2826 (1965).

45. R.D. Shannon, Acta Crystallogr. A32 751-767 (1976).

46. M. German, L.M. Kovba, and K. Shturm, Russ. J. Inorg. Chem., 29 1257-1260 (1984).

47. M. German and L.M. Kovba, Russ. J. Inorg. Chem., 30 1204-1207 (1985).

48. Powder Diffraction File, Joint Committee for Powder Diffraction Standards, Swarthmore, PA, Card No. 35-734 (1990).

49. B.D. Cullity, Elements of X-ray Diffraction, Addison-Wesley Publishing Co., Inc., Reading, Massachusetts, (1978).

50. H.P. Rooksby, E.A.D. White, and S.A. Langston, J. Amer. Ceram. Soc., 48 447-449 (1965).

51. P.E. Fielding and T.J. White, J. Mater. Res. 2 387-414 (1987).

52. D.R. Clarke, Ann. Rev. Mater. Sci. 13 191-218 (1983).

53. E.R. Vance, P.J. Angel, B.D. Begg, and R.A. Day, Scientific Basis for Nuclear Waste Management XV, Mat. Res. Soc. Symp. Proc. Vol. 333, eds. R.C. Ewing, Materials Research Society, Pittsburgh, PA, 293-298 (1994).

54. T.J. White and J. Mitamura, Scientific Basis for Nuclear Waste Management XVI, Mat. Res. Soc. Symp. Proc. Vol. 294, eds. C.G. Interrante and R.T. Pabalan, Materials Research Society, Pittsburgh, PA, 109-116 (1993).

55. F.W. Clinard, Jr., L.W. Hobbs, C.C. Land, D.E. Peterson, D.L. Rohr, and R.B. Roof, J. Nucl. Mater. 105 248-256 (1982).

56. A. Tabuteau and M. Pagés, The Handbook on the Physics and Chemistry of the Actinides, eds. A.J. Freeman and C. Keller, Elsevier Science Publishers, Amsterdam, 185-241 (1985).

57. R.S. Roth, J. Res. Natl. Bur. Stand. 58 75-88 (1957).

58. E. Johnson, personal communication, Oak Ridge National Laboratory, Chemical and Analytical Sciences Division, Oak Ridge, TN 37831-6375 (1995).

59. M.A. Subramanian and A.W. Sleight, The Handbook on the Physics and Chemistry of the Rare Earths, eds. K.A. Gschneidner, Jr. and L. Eyring, Elsevier Science Publishers, Amsterdam, 225-248 (1993).

60. J.J. Casey, L. Katz, and W.C. Orr, J. Am. Chem. Soc., 77 2187-2189 (1955).

APPENDIX

AUXILIARY CALCULATIONS

A. Gravimetric Relationships

For the compound $Ln_2O_3 \cdot (nTiO_{2-m})$ (Ln=La, Pr, or Nd), the weight gain achieved by air oxidation can be used to estimate the value of m, proportional to the oxidation of Ti(III) to Ti(IV), following the example calculation given below.

$$Ln_2O_3 \cdot (nTiO_{2-m}) + 0.5nmO_2 \text{ ---> } Ln_2O_3 \cdot (nTiO_2) \qquad \text{(A1)}$$

If %G = the weight gain expressed as a percent,
n = moles of titanium present,
FW = formula weight of the compound if complete oxidation is achieved, i.e., for $Ln_2O_3 \cdot (nTiO_2)$

$$\%G = \frac{(0.5nm)x32x100}{FW-(0.5nm)x32} = \frac{1600nm}{FW-16nm} \qquad \text{(A2)}$$

$$m = \frac{\%G(FW)}{16n[\%G+100]} \qquad \text{(A3)}$$

Example: 1.48% weight gain measured for $La_2O_3 \cdot (3.5TiO_{2-m})$,
FW = 605.47 g/mol
n = 3.5

Using these values in (A3):

$$m = \frac{(1.48)(605.47)}{16(3.5)[1.48+100]}$$

$$m = 0.16$$

For the compound $Pu_2O_3 \cdot (3TiO_{2-m})$, the weight gain achieved by air oxidation is proportional to the oxidation of Pu(III) to Pu(IV) in addition to the oxidation of Ti(III) to Ti(IV).

$$Pu_2O_3 \cdot (nTiO_{2-m}) + (0.5 + 0.5nm)O_2 \longrightarrow 2PuO_2 + nTiO_2 \quad (A4)$$

If %G = the weight gain expressed as a percent,
n = moles of titanium present,
FW = formula weight of the compound if complete oxidation is achieved, i.e., for $2PuO_2 + nTiO_2$

$$\%G = \frac{(0.5+0.5nm)x32x100}{FW-(0.5+0.5nm)x32} \quad (A5)$$

$$m = \frac{\%G(FW)-1600-16\%G}{n[1600+16\%G]} \quad (A6)$$

Example: 2.6% weight gain measured for $Pu_2O_3 \cdot (3TiO_{2-m})$,
FW = 755.7 g/mol
n = 3

Using the values in (A6):

$$m = \frac{(2.6)(755.70)-1600-16(2.6)}{3[1600+16(2.6)]}$$

$$m = 0.07$$

B. Mass and Charge Balance Equations to Determine the Composition of $Sr_{4-x}Ln_{2x/3}Ti_4O_{12}$ When Obtained Together with $Ln_2Ti_2O_7$

For example, a preparation containing, in mol percent, 15% SrO, 30% $PrO_{1.5}$, and 55% TiO_2 showed, by XRD, the presence of the cubic (slightly distorted to tetragonal) perovskite-type, $Sr_{4-x}Pr_{2x/3}Ti_4O_{12}$, and $Pr_2Ti_2O_7$. The solutions of a system of simultaneous equations of mass and charge balance allowed for estimating the values of a, b, and x in the following equation:

$$Sr_{1.09}Pr_{2.18}Ti_4O_{12.36} \text{ ---> } aPr_2Ti_2O_7 + bSr_{4-x}Pr_{2x/3}Ti_4O_{12} \qquad \text{(A7)}$$

Substituting c for 4-x and d for 2x/3 ($Sr_cPr_dTi_4O_{12}$), the following mass balance equations can be defined:

Pr $2a + bd = 2.18$ (A8)

Sr $bc = 1.09$ (A9)

Ti $2a + 4b = 4$ (A10)

The following charge balance equation for the strontium and the praseodymium in the perovskite can be defined:

$2c + 3d = 8$ (A11)

Now there is a system of four equations and four unknowns which can be solved.

$$\begin{aligned} 2a + 4b &= 4 \\ -(2a + bd &= 2.18) \\ 4b - bd &= 1.82 \end{aligned}$$

$b(4 - d) = 1.82$; $b = 1.09/c$

$1.09/c(4-d) = 1.82$

$4.36/c - 1.09d/c = 1.82$

$1.82c + 1.09d = 4.36$

$$\begin{array}{r} 1.82c + 1.09d = 4.36 \\ -0.363(2c + 3d = 8) \end{array} \qquad \begin{array}{r} 1.82c + 1.09d = 4.36 \\ -0.73c + 1.09d = 2.90 \\ 1.09c = 1.46 \\ c = 1.34 \end{array}$$

Therefore, by substitution back into the original four equations (A8-11), the values of a, b, and d are obtained: a=0.38, b=0.81, and d=1.77. This yields a perovskite-type phase of composition $Sr_{1.34}Pr_{1.77}Ti_4O_{12}$, thus containing 18.8 mol percent SrO. The measured formula unit volume of this perovskite-type phase was plotted in Figure 8 (p. 53) versus the empirically calculated SrO content.

C. Mass Balance Equations to Attempt to Verify the Estimated Compositions of $SrNd_2Ti_{4-y}Zr_yO_{12}$ and $Nd_aTi_bZr_cO_7$

Attempts to replace titanium by zirconium in $SrNd_2Ti_4O_{12}$ resulted in a multi-phase product which included a perovskite-type phase and a pyrochlore-type phase. Compositions of the perovskite-type phase, assuming no substitution of zirconium for titanium in this phase, were estimated based on the measured volume in comparison to Figure 8. Compositions of the pyrochlore-type mixed titanium-zirconium phase were estimated based on the measured volume of the phase and compounds of known composition with a similar volume. Using mass balance calculations, the compositions of these two phases were attempted to be verified based on the original composition

of the preparation.

Example: Attempts to prepare $SrNd_2Ti_{3.2}Zr_{0.8}O_{12}$ resulted in the formation of a perovskite-type phase, a pyrochlore-type phase, and ZrO_2. Using the volume of the perovskite-type phase and Figure 8, the perovskite was estimated to contain approximately 30.8 mol percent SrO. The following calculation was used to determine the composition of the perovskite-type phase $Sr_{4-x}Nd_{2x/3}Ti_4O_{12}$:

$$\frac{4-x}{4-x+\frac{2x}{3}+4}=0.308 \qquad \text{(A12)}$$

$$x=1.71$$

Therefore, the estimated composition of the perovskite-type phase was $Sr_{2.29}Nd_{1.14}Ti_4O_{12}$. The composition of the pyrochlore-type phase was estimated to be $Nd_{1.70}Ti_{0.85}Zr_{1.38}O_7$ based on its volume. Using these estimated compositions and the knowledge that ZrO_2 was also present, the following equation results:

$$SrNd_2Ti_{3.2}Zr_{0.8} \text{ ---->} aSr_{2.29}Nd_{1.14}Ti_4O_{12} + bNd_{1.70}Ti_{0.85}Zr_{1.38}O_7 + cZrO_2 \qquad \text{(A13)}$$

Attempts to balance this equation were unsuccessful, as the coefficient for c is negative.

Sr $2.29a = 1$ (A14)

$a = 0.44$

Nd $1.14a + 1.7b = 2$ (A15)

$1.14(0.44) + 1.7b = 2$

$b=0.88$

Zr $1.38b + c = 0.8$ (A16)

$1.38(0.88) + c = 0.8$

$c = -0.41$

Therefore, the compositions estimated are incorrect, indicating that there could have been some substitution of zirconium for titanium in the perovskite-type phase or that the pyrochlore-type compound $Nd_aTi_bZr_cO_7$ has a different composition from the phases studied here.

VITA

Shara Leeann Stoddard [redacted] She graduated co-salutatorian from Hixson High School in 1988 and entered the University of Tennessee at Chattanooga that fall. There she was a Grote Chemistry Scholar and participated in the summer research program for two years. In the spring of 1991, Shara was awarded a Bachelor of Science Degree, Magna Cum Laude, Highest Honors in Chemistry. Following graduation, she entered the Ph.D. program in chemistry at the University of Tennessee at Knoxville and was selected to be a Dupont Fellow. During her first one-and-a-half years at Knoxville, she served as a full- or part-time teaching assistant for the chemistry department, while the remainder of her time was served as a graduate research assistant at the Oak Ridge National Laboratory. During her undergraduate and graduate schooling, Shara has presented research papers at three American Chemical Society meetings and has co-authored several papers appearing in the Journal of Alloys and Compounds and the Journal of the American Ceramic Society. On June 20, 1992, Shara married Ryan Frederick Shoup.